Structural and Electronic Variations of sp/sp^2 Carbon-Based Bridges in Di- and Trinuclear Redox-Active Iron Complexes Bearing $Fe(diphosphine)_2X$ (X = I, NCS) Moieties

Franziska Lissel, Olivier Blacque, Koushik Venkatesan and Heinz Berke*

† Department of Chemistry, University of Zurich, Winterthurerstrasse 190, CH-8057 Zurich, Switzerland

* hberke@chem.uzh.ch

General Procedures

Reagent grade toluene, pentane, diethyl ether and tetrahydrofuran were dried and distilled from sodium prior to use. Reagent grade benzene and dichloromethane were dried and distilled from CaH_2, acetonitrile from P_2O_5. Deuterated solvents were dried and distilled likewise.

The stannylated linkers 1,4-bis((trimethylstannylethynyl)benzene, 1,3-bis((trimethylstannyl)ethynyl)benzene, 4,4'-bis((trimethylstannyl)ethynyl)biphenyl, 2,5-bis((trimethylstannyl)ethynyl)thiophene and 1,3,5-tris((trimethylstannyl)ethynyl)benzene were obtained by lithiating the corresponding deprotected alkynes at low temperature and then reacting them with stochiometric amounts of Me_3SnCl. The stannylated reagents were purified by two subsequent crystallizations from cold pentane. *Trans*-$Fe(depe)_2I_2$ was synthesized as described in literature.[1] Commercially available NaSCN was recrystallized from methanol prior to use.

NMR spectra were measured on a on a Bruker Biospin at 500 MHz for ^1H, 125.8 MHz for $^{13}C\{^1H\}$ and 202.5 MHz for $^{31}P\{^1H\}$. Chemical shifts for ^1H and ^{13}C are given in ppm relative to the solvent[2] and for ^{31}P relative to phosphoric acid. All NMR spectra were recorded at room temperature. IR spectra were measured using an ATR bridge and recorded on a Perkin-Elmer Spectrum Two FT-IR spectrometer. Raman spectra were recorded on a Renishaw Ramanscope spectrometer (514 nm). CHN elemental analyses were performed with a LECO CHN-932 microanalyzer. Cyclic voltammograms were obtained with a BAS 100W Voltammetric Analyzer (low volume cell). The cell was equipped with an Au working electrode and a Pt counter electrode, and an Ag reference electrode. All sample solutions were 0.1M in Bu_4NPF_6 and recorded with a scan rate of 100 mV/s. Ferrocene was used as an external standard. A BAS 100W program was employed for the data analysis.

Syntheses

[I–(depe)$_2$Fe–1,4–(C≡C–C$_6$H$_4$–C≡C)–Fe(depe)$_2$–I] 1

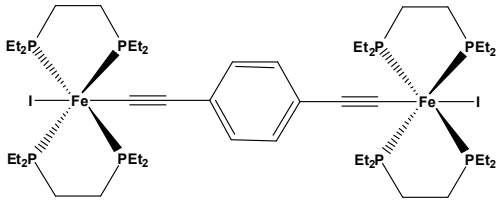

Trans-Fe(depe)$_2$I$_2$ (289 mg, 0.4 mmol) and 1,4-bis((trimethylstannyl)ethynyl)benzene (95 mg, 0.21 mmol) were suspended in THF (10 mL) and heated to reflux for 12 h. The THF was removed *in vacuo* and the obtained solid washed with pentane/diethyl ether (1:1, 3 x 10 mL). The product was extracted with toluene (40 mL) and the solution filtered over diatomite. Drying *in vacuo* gave the title compound as a red solid.

Yield: 228 mg = 0.173 mmol = 86.7 %.

Crystals suitable for X-ray were grown by slow diffusion of pentane into a THF solution at rt.

Anal. Calcd.: C: 45.68; H: 7.67. **Found**: C: 45.91; H: 7.51. **IR** (ATR, cm^{-1}): 2028 (vs, $\nu_{C\equiv C}$); 1489 (m, $\nu_{C=C}$). **Raman** (cm^{-1}): 2030 (m, $\nu_{C\equiv C}$); 1586 (s, $\nu_{C=C}$). **^{1}H NMR** (500 MHz, THF-d$_8$): δ = 6.50 (s, 4H, Ar-**H**), 2.62 - 2.53 (m, 8H, C**H**$_2$-CH$_3$), 2.47 - 2.38 (m, 8H, C**H**$_2$-CH$_3$), 2.06 - 1.89 (m, 24H, C**H**$_2$-CH$_3$ and C**H**$_2$-CH$_2$), 1.83 - 1.75 (m, 8H, C**H**$_2$-CH$_3$, overlapping with THF), 1.26 - 1.14 (m, 48H, CH$_2$-C**H**$_3$). **^{13}C{^{1}H} NMR** (125.8 MHz, THF-d$_8$): δ = 129.9 (s, *o*-**C**), 125.6 (s, *i*-**C**), 124.15 (s, Fe-C≡**C**), 122.7 (p, $^2J_{C\text{-}P}$ = 23.9 Hz, Fe-**C**≡C), 25.1 - 24.9 (m, **C**H$_2$-CH$_3$), 22.6 - 22.1 (m, **C**H$_2$-**C**H$_2$), 21.3 - 21.1 (m, **C**H$_2$-CH$_3$), 10.5 (d, $^2J_{C\text{-}P}$ = 75.5 Hz, CH$_2$-**C**H$_3$). **^{31}P{^{1}H} NMR** (202.5 MHz, THF-d$_8$): δ = 66.0 (s).

[I–(depe)$_2$Fe–1,3–(C≡C–C$_6$H$_4$–C≡C)–Fe(depe)$_2$–I] 2

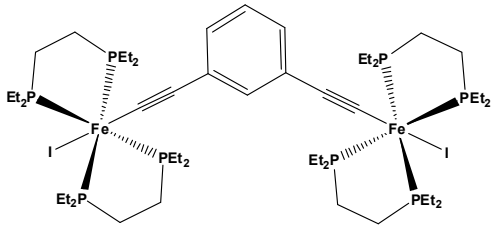

Trans-Fe(depe)$_2$I$_2$ (289 mg, 0.4 mmol) and 1,3-bis((trimethylstannyl)ethynyl)benzene (95 mg, 0.21 mmol) were suspended in THF (10 mL) and heated to reflux for 12 h. The THF was removed in vacuo and the obtained pink solid washed with pentane (3 x 10 mL). The product was extracted with benzene (25 mL) and the solution filtered over a patch of diatomite. Drying *in vacuo* gave the title compound as a pink solid.

Yield: 238 mg = 0.181 mmol = 90.5 %.

Crystals suitable for X-ray were grown by slow diffusion of pentane into a THF solution at rt.

Anal. Calcd.: C: 45.68; H: 7.67. **Found**: C: 45.49; H: 7.53. **IR** (ATR, cm^{-1}): 2036 (vs, $\nu_{C\equiv C}$); 1571 (s, $\nu_{C=C}$); 1551 (m, $\nu_{C=C}$). **Raman** (cm^{-1}): 2040 (s, $\nu_{C\equiv C}$); 1574 (m, $\nu_{C=C}$). **^{1}H NMR** (500 MHz, THF-d_8): δ = 6.62 (t, 1H, $^3J_{H-H}$ = 7.5 Hz, 5-Ar-**H**), 6.39 (s, 1H, 2-Ar-**H**), 6.31 (d, 1H, $^3J_{H-H}$ = 7.5 Hz, 4-Ar-**H**), 2.64 - 2.54 (m, 8H, C**H**$_2$-CH$_3$), 2.50 - 2.38 (m, 8H, C**H**$_2$-CH$_3$), 2.06 - 1.88 (m, 24H, C**H**$_2$-CH$_3$ and C**H**$_2$-CH$_2$), 1.83 - 1.75 (m, 8H, C**H**$_2$-CH$_3$), 1.26 - 1.14 (m, 48H, CH$_2$-C**H**$_3$). **^{13}C{^{1}H} NMR** (125.8 MHz, THF-d_8): δ = 132.1 (s, 2-Ar-**C**), 130.9 (p, $^2J_{C-P}$ = 37.7 Hz, Fe-**C**≡C), 130.6 (s, 1-Ar-**C**), 127.9 (s, 5-Ar-**C**), 124.9 (s, 4-Ar-**C**), 123.8 (Fe-C≡**C**), 25.1 - 24.8 (m, **C**H$_2$-CH$_3$) 22.5 - 22.0 (m, **C**H$_2$-**C**H$_2$), 21.3 - 20.9 (m, **C**H$_2$-CH$_3$), 10.6 (d, $^2J_{C-P}$ = 62.9 Hz, CH$_2$-**C**H$_3$). **^{31}P{^{1}H} NMR** (202.5 MHz, THF-d_8): δ = 66.1 (s).

[I–(depe)$_2$Fe–4,4–(C≡C–C$_6$H$_4$–C$_6$H$_4$–C≡C)–Fe(depe)$_2$–I] 3

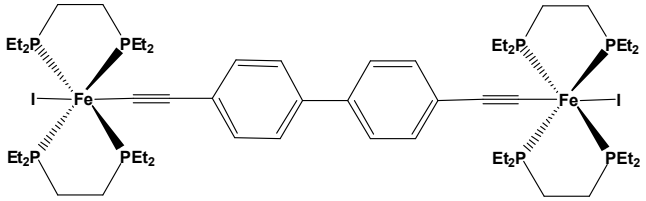

Trans-Fe(depe)$_2$I$_2$ (289 mg, 0.4 mmol) and 4,4'-bis((trimethylstannyl)ethynyl)biphenyl (110 mg, 0.208 mmol) were suspended in THF (10 mL) and heated to reflux for 12 h. After cooling down to rt, a yellow-orange precipitate formed. Pentane (30 mL) was added and the supernatant solution removed. The precipitate was washed with pentane (3 x 10 mL). After extraction with hot toluene (90°C, 40 mL), the solution was filtered hot over a patch of diatomite. The toluene was removed *in vacuo* to give the title compound as an orange solid.

Yield: 251 mg = 0.181 mmol = 90.4 %.

Anal. Calcd.: C: 48.36; H: 7.54. **Found**: C: 48.56; H: 7.55. **IR** (ATR, cm^{-1}): 2023 (vs, $\nu_{C\equiv C}$); 1595 (m, $\nu_{C=C}$); 1480 (s, $\nu_{C=C}$). **Raman** (cm^{-1}): 2040 (w, $\nu_{C\equiv C}$); 1591 (vs, $\nu_{C=C}$). **^{1}H NMR** (500 MHz, CD_2Cl_2): δ = 7.23 (d, 4H, $^3J_{H-H}$ = 10.0 Hz, Ar-**H**), 6.88 (d, 4H, $^3J_{H-H}$ = 10.0 Hz, Ar-**H**), 2.63 - 2.51 (m, 8H, C**H**$_2$-CH$_3$), 2.10 - 1.90 (m, 24 H, C**H**$_2$-CH$_3$ and C**H**$_2$-CH$_2$), 1.88 - 179 (m, 8H, C**H**$_2$-CH$_3$), 1.32 - 1.17 (m, 48H, CH$_2$-C**H**$_3$). **^{13}C{^{1}H} NMR** (125.8 MHz, CD_2Cl_2): δ = 135.0 (s, Ar-**C**), 130.3 (s, Ar-**C**-H), 128.6 (s, Ar-**C**), 126.1 (s, Ar-**C**-H), 123.3 (s, Fe-C≡**C**), 24.4 - 24.0 (m, **C**H$_2$-CH$_3$) 21.8 - 21.3 (m, **C**H$_2$-**C**H$_2$), 20.5 - 20.2 (m, **C**H$_2$-CH$_3$), 10.3 (d, $^2J_{C-P}$ = 75.5 Hz, CH$_2$-**C**H$_3$). **^{31}P{^{1}H} NMR** (202.5 MHz, CD_2Cl_2): δ = 64.8 (s).

[I–(depe)$_2$Fe–2,5–(C≡C–SC$_4$H$_2$–C≡C)–Fe(depe)$_2$–I] 4

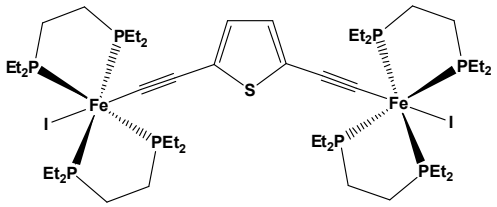

Trans-Fe(depe)$_2$I$_2$ (289 mg, 0.4 mmol) and 2,5-bis((trimethylstannyl)ethynyl)thiophene (96 mg, 0.21 mmol) were suspended in toluene (10 mL) and heated to 80°C for 12 h. After cooling down, the brown solution was concentrated to 5 mL before pentane was added (20 mL), causing a precipitate to form. The supernatant solution was removed and the precipitate washed with pentane (3 x 10 mL). The product was extracted with benzene (20 mL) and the solution filtered over a patch of diatomite. Drying *in vacuo* gave the title compound as a brown solid.

Yield: 234 mg = 0.177 mmol = 88.4 %.

Crystals suitable for X-ray were grown in benzene/pentane at rt.

Anal. Calcd.: C: 43.65; H: 7.48. **Found**: C: 43.81; H: 7.51. **IR** (ATR, cm^{-1}): 2034 (s, $\nu_{C\equiv C}$); 1502 (w, $\nu_{C=C}$). **Raman** (cm^{-1}): 2032 (m, $\nu_{C\equiv C}$); 1439 (vs, $\nu_{C=C}$). **^{1}H NMR** (500 MHz, C_6D_6): δ = 6.38 (s, 2H, 3-Thiophene-**H**), 2.72 - 2.62 (m, 8H, C**H**$_2$-CH$_3$), 2.44 - 2.33 (m, 8H, C**H**$_2$-CH$_3$), 1.92 - 1.79 (m, 16H, C**H**$_2$-CH$_3$ and C**H**$_2$-CH$_2$), 1.77 - 1.61 (m, 16H, C**H**$_2$-CH$_3$ and C**H**$_2$-CH$_2$), 1.11 - 1.02 (m, 48H, CH$_2$-C**H**$_3$). **^{13}C{^{1}H} NMR** (125.8 MHz, C_6D_6): δ = 137.6 (p, $^2J_{C\text{-}P}$ = 28.9 Hz, Fe-**C**≡C), 125.4 (s, Fe-C≡**C**), 123.1 (s, 3-Thiophene-**C**), 115.4 (s, 2-Thiophene-**C**), 24.5 - 24.3 (m, **C**H$_2$-CH$_3$), 22.0 - 21.5 (m, **C**H$_2$-**C**H$_2$), 20.9 - 20.6 (m, **C**H$_2$-CH$_3$), 10.3 (d, $^2J_{C\text{-}P}$ = 62.9 Hz, CH$_2$-**C**H$_3$). **^{31}P{^{1}H} NMR** (202.5 MHz, C_6D_6): δ = 67.9 (s).

[{I–(depe)$_2$Fe–C≡C–}$_3$–(1,3,5–C$_6$H$_3$)] 5

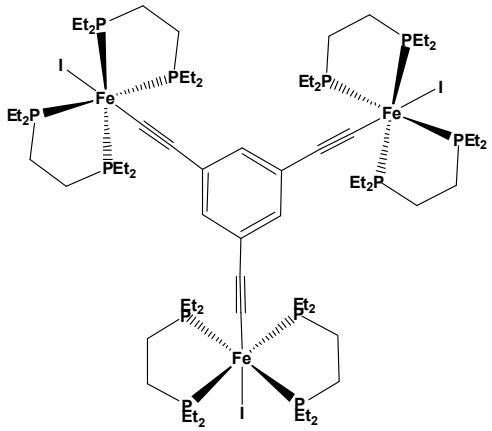

Trans-Fe(depe)$_2$I$_2$ (217 mg, 0.3 mmol) and 1,3,5-tris((trimethylstannyl)ethynyl)benzene (67 mg, 0.105 mmol) were suspended in THF (50 mL) and heated to reflux for 12 h. The red solution was then filtered hot over a patch of diatomite and concentrated to a volume of 20 mL, causing a pink precipitate to form. The supernatant solution was removed and the precipitate washed with diethyl ether (3 x 10 mL). Drying *in vacuo* gave the title compound as a pink solid.

Yield: 180 mg = 0.0931 mmol = 93.1 %.

Anal. Calcd.: C: 44.74; H: 7.67. **Found**: C: 44.95; H: 7.46. **IR** (ATR, cm^{-1}): 2046 (vs, $\nu_{C\equiv C}$); 1551 (vs, $\nu_{C=C}$). **Raman** (cm^{-1}): 2049 (s, $\nu_{C\equiv C}$); 1561 (m, $\nu_{C=C}$). **^{1}H NMR** (500 MHz, CD_2Cl_2): δ = 5.94 (s, 3H, Ar-**H**)**,** 2.55 - 2.44 (m, 12H, C**H**$_2$-CH$_3$), 2.40 - 2.27 (m, 12H, C**H**$_2$-CH$_3$), 2.00 - 1.84 (m, 32H, C**H**$_2$-CH$_3$ and C**H**$_2$-CH$_2$), 1.76 - 1.67 (m, 12H, C**H**$_2$-CH$_3$), 1.20 - 1.12 (m, 72H, CH$_2$-C**H**$_3$). **^{13}C{^{1}H} NMR** (125.8 MHz, CD_2Cl_2): δ = 126.3 (s, Ar-**C**-H), 24.8 - 24.2 (m, **C**H$_2$-CH$_3$), 22.1 - 21. 5 (m, **C**H$_2$-**C**H$_2$), 20.7 - 20.1 (m, **C**H$_2$-CH$_3$), 10.4 (d, $^2J_{C\text{-}P}$ = 75.5 Hz, CH$_2$-**C**H$_3$). **^{31}P{^{1}H} NMR** (202.5 MHz, CD_2Cl_2): δ = 66.5 (s).

[SCN–(depe)$_2$Fe–1,4–(C≡C–C$_6$H$_4$–C≡C)–Fe(depe)$_2$–NCS] 6

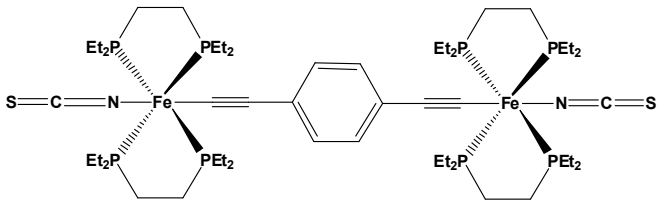

Compound **1** (66 mg, 0.05 mmol) and NaSCN (81 mg, 1 mmol) were dispersed in acetonitrile (15 mL) and heated to reflux for 12 h. Complex **1** gradually dissolved to give a yellow solution. The solution was concentrated to 5 mL, causing a yellow precipitate to form. The precipitate was filtered off using a patch of diatomite and washed with acetonitrile (3 x 5 mL). The product, a yellow solid, was extracted with benzene (40 mL) and dried *in vacuo*.

Yield: 54.1 mg = 0.046 mmol = 92.0 %.

Crystals suitable for X-ray were grown by slow diffusion of pentane into a THF solution at rt.

Anal. Calcd.: C: 53.06; H: 8.56; N: 2.38. **Found**: C: 52.80; H: 8.61; N: 2.42. **IR** (ATR, cm^{-1}): 2092 (s, $\nu_{C=N}$); 2044 (s, $\nu_{C\equiv C}$); 1489 (m, $\nu_{C=C}$). **Raman** (cm^{-1}): 2043 (m, $\nu_{C\equiv C}$); 1590 (s, $\nu_{C=C}$). **^{1}H NMR** (500 MHz, CD_2Cl_2): δ = 6.50 (s, 4H, Ar-**H**), 2.29 - 2.20 (m, 8H, C**H**$_2$-CH$_3$), 1.95 - 1.72 (m, 40H, C**H**$_2$-CH$_3$ and C**H**$_2$-CH$_2$), 1.24 - 1.14 (m, 48H, CH$_2$-C**H**$_3$). **^{13}C{^{1}H} NMR** (125.8 MHz, CD_2Cl_2): δ = 139.5 (s, Fe-N=**C**=S), 129.6 (s, *o*-**C**), 127.7 (p, $^2J_{C-P}$ = 25.2 Hz, Fe-**C**≡C), 124.9 (s, *i*-**C**), 120.6 (s, Fe-C≡**C**), 21.3 - 20.7 (m, **C**H$_2$-CH$_3$), 20.0 - 19.6 (m, **C**H$_2$-**C**H$_2$ and **C**H$_2$-CH$_3$), 9.5 (d, $^2J_{C-P}$ = 37.7 Hz, CH$_2$-**C**H$_3$). **^{31}P{^{1}H} NMR** (202.5 MHz, CD_2Cl_2): δ = 73.8 (s).

[SCN–(depe)$_2$Fe–1,3–(C≡C–C$_6$H$_4$–C≡C)–Fe(depe)$_2$–NCS] 7

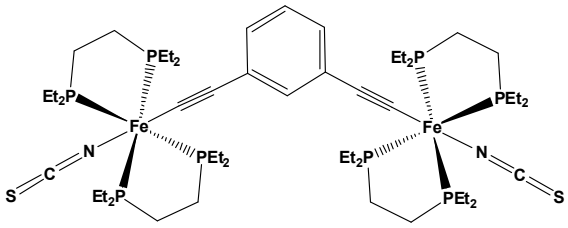

Compound **2** (66 mg, 0.05 mmol) and NaSCN (81 mg, 1 mmol) were dispersed in acetonitrile (15 mL) and heated to reflux for 5 h, yielding a yellow solution. The acetonitrile was removed *in vacuo* and the resulting solid washed with diethyl ether (3 x 5 mL). The product extracted with benzene/pentane (2:1, 40 mL). The solution was filtered over a patch of diatomite. Drying *in vacuo* gave the title compound as yellow solid.

Yield: 53.6 mg = 0.0455 mmol = 91.1 %.

Anal. Calcd.: C: 53.06; H: 8.56; N: 2.38. **Found**: C: 53.31; H: 8.47; N: 2.15. **IR** (ATR, cm^{-1}): 2092 (s, $\nu_{C=N}$); 2041 (vs, $\nu_{C\equiv C}$); 1574 (s, $\nu_{C=C}$); 1552 (m, $\nu_{C=C}$). **Raman** (cm^{-1}): 2097 (m, $\nu_{C=N}$); 2040 (vs, $\nu_{C\equiv C}$); 1578 (m, $\nu_{C=C}$); 1552 (w, $\nu_{C=C}$). **^{1}H NMR** (500 MHz, THF-d_8): δ = 6.59 (t, 1H, $^3J_{H-H}$ = 7.5 Hz, 5-Ar-**H**), 6.35 (s, 1H, 2-Ar-**H**), 6.31 (d, 1H, $^3J_{H-H}$ = 10.0 Hz, 4-Ar-**H**), 2.38 - 2.26 (m, 8H, C**H**$_2$-CH$_3$), 2.00- 1.79 (m, 40H, C**H**$_2$-CH$_3$ and C**H**$_2$-CH$_2$), 1.27 - 1.18 (m, 48H, CH$_2$-C**H**$_3$). **^{13}C{^{1}H} NMR** (125.8 MHz, THF-d_8): δ = 142.8 (s, Fe-N=**C**=S), 132.3 (s, 2-Ar-**C**), 130.3 (s, 1-Ar-**C**), 127.9 (s, 5-Ar-**C**), 126.8 (p, $^2J_{C-P}$ = 25.2 Hz, Fe-

C≡C), 125.2 (s, 4-Ar-**C**), 121.1 (Fe-C≡**C**), 21.8 - 21.3 (m, **C**H_2-CH_3) 20.8 - 20.5 (m, **C**H_2-**C**H_2), 20.4 - 20.2 (m, **C**H_2-CH_3), 9.7 (d, $^2J_{C-P}$ = 50.3 Hz, CH_2-**C**H_3). **^{31}P{^{1}H} NMR** (202.5 MHz, THF-d_8): δ = 74.4 (s).

[SCN–(depe)$_2$Fe–4,4'–(C≡C–C_6H_4–C_6H_4–C≡C)–Fe(depe)$_2$–NCS] 8

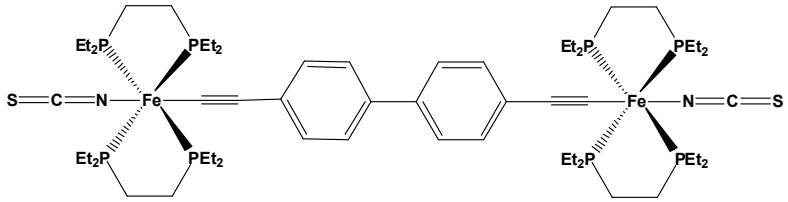

Compound **3** (70 mg, 0.05 mmol) and NaSCN (81 mg, 1 mmol) were dispersed in acetonitrile (15 mL) and heated to reflux for 12 h. The components never fully dissolved over the course of the reaction, a yellow precipitate was always present. The solution was concentrated to 5 mL to promote further precipitation. The solid was filtered off using a patch of diatomite and washed with acetonitrile (3 x 5 mL). The product, a yellow-orange solid, was extracted with benzene (40 mL) and dried *in vacuo*.

Yield: 58 mg = 0.047 mmol = 93.2 %.

Crystals suitable for X-ray were grown by slow evaporation of a THF/acetonitrile solution at rt.

Anal. Calcd.: C: 55.59; H: 8.37; N: 2.24. **Found**: C: 55.78; H: 8.31; N: 2.16. **IR** (ATR, cm^{-1}): 2094 (s, $\nu_{C\equiv N}$); 2034 (vs, $\nu_{C\equiv C}$); 1596 (s, $\nu_{C=C}$); 1481 (s, $\nu_{C=C}$). **Raman** (cm^{-1}): 2045 (w, $\nu_{C\equiv C}$); 1591 (vs, $\nu_{C=C}$); 1522 (vw, $\nu_{C=C}$). **^{1}H NMR** (500 MHz, CD_2Cl_2): δ = 7.19 (d, 4H, $^3J_{H-H}$ = 8.0 Hz, Ar-**H**), 6.84 (d, 4H, $^3J_{H-H}$ = 8.0 Hz, Ar-**H**), 2.37 - 2.25 (m, 8H, C**H**$_2$-CH_3), 2.06 - 1.75 (m, 40H, C**H**$_2$-CH_3 and C**H**$_2$-CH_2), 1.30 - 1.13 (m, 48H, CH_2-C**H**$_3$). **^{13}C{^{1}H} NMR** (125.8 MHz, CD_2Cl_2): δ = 139.9 (s, Fe-N=**C**=S), 135.5 (s, Ar-**C**), 132.2 (p, $^2J_{C-P}$ = 28.3 Hz, Fe-**C**≡C), 130.4 (s, Ar-**C**-H), 128.7 (s, Ar-**C**), 126.2 (s, Ar-**C**-H), 120.3 (s, Fe-C≡**C**), 21.4 - 21.0 (m, **C**H_2-CH_3) 20.2 - 19.9 (m, **C**H_2-**C**H_2), 19.9 - 19.7 (m, **C**H_2-CH_3), 9.6 (d, $^2J_{C-P}$ = 62.9 Hz, CH_2-**C**H_3). **^{31}P{^{1}H} NMR** (202.5 MHz, CD_2Cl_2): δ = 73.9 (s).

[SCN–(depe)$_2$Fe–2,5–(C≡C–SC_4H_2–C≡C)–Fe(depe)$_2$–NCS] 9

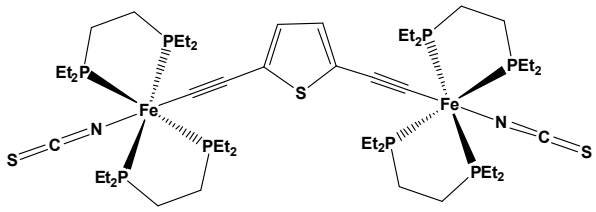

Compound **4** (66 mg, 0.05 mmol) and NaSCN (81 mg, 1 mmol) were dispersed in acetonitrile (15 mL) and heated to reflux for 12 h, yielding a brown solution. The acetonitrile was removed *in vacuo* and the resulting solid washed with cold diethyl ether (-20°C, 3 x 5 mL). Then the product was extracted with benzene/pentane (2:1; 40 mL). The solution was filtered over a patch of diatomite. Drying *in vacuo* gave the title compound as yellow-brown solid.

Yield: 57 mg = 0.049 mmol = 97.0 %

Crystals suitable for X-ray were grown by slow diffusion of pentane into a benzene solution at rt.

Anal. Calcd.: C: 50.76; H: 8.35; N: 2.37. **Found**: C: 50.71; H: 8.31; N: 2.30. **IR** (ATR, cm^{-1}): 2094 (s, $\nu_{C=N}$); 2031 (s, $\nu_{C\equiv C}$); 1503 (w, $\nu_{C=C}$). **Raman** (cm^{-1}): 2097 (w, $\nu_{C=N}$); 2036 (m, $\nu_{C\equiv C}$); 1434 (vs, $\nu_{C=C}$). **^{1}H NMR** (500 MHz, C_6D_6): δ = 6.24 (s, 2H, 4-Thiophene-**H**), 2.14 - 2.07 (m, 8H, C**H**$_2$-CH$_3$), 1.90 - 1.83 (m, 8H, C**H**$_2$-CH$_3$), 1.61 - 1.45 (m, 32H, C**H**$_2$-CH$_3$ and C**H**$_2$-CH$_2$), 1.03 - 0.94 (m, 48H, CH$_2$-C**H**$_3$). **^{13}C{^{1}H} NMR** (125.8 MHz, C_6D_6): δ = 142.5 (2, Fe-N=**C**=S), 133.6 (p, $^2J_{C-P}$ = 25.2 Hz, Fe-C≡**C**), 125.2 (s, 3-Thiophene-**C**), 123.4 (s, Fe-C≡**C**), 112.5 (s, 2-Thiophene-**C**), 21.1 - 20.0 (m, **C**H$_2$-CH$_3$), 20.0 - 19.7 (m, **C**H$_2$-**C**H$_2$), 19.7 - 19.5 (m, **C**H$_2$-CH$_3$), 9.3 (d, $^2J_{C-P}$ = 37.7 Hz, CH$_2$-**C**H$_3$). **^{31}P{^{1}H} NMR** (202.5 MHz, C_6D_6): δ = 74.0 (s).

[{SCN–(depe)$_2$Fe–C≡C–}$_3$–(1,3,5–C$_6$H$_3$)] 10

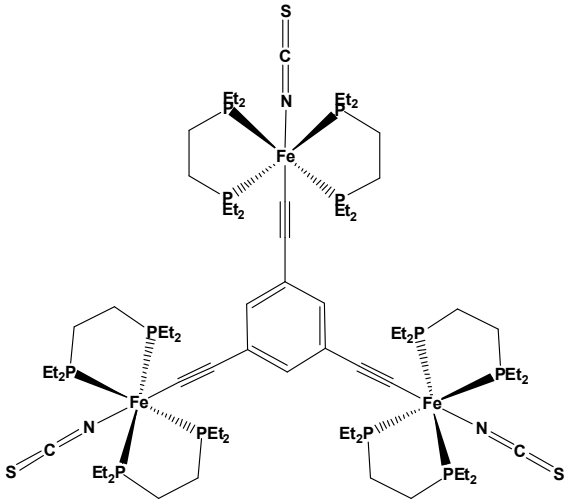

Compound **5** (97 mg, 0.05 mmol) and NaSCN (122 mg, 1.5 mmol) were dispersed in acetonitrile (15 mL) and heated to reflux for 5 h. The pink complex **5** gradually dissolved to give a yellow solution. The solution was concentrated to 5 mL, causing a yellow precipitate to form. The precipitate was filtered off using a patch of diatomite and washed with acetonitrile (3 x 5 mL). The product, a yellow solid, was extracted with benzene (40 mL) and dried *in vacuo*.

Yield: 83 mg = 0.048 mmol = 96.2%.

Anal. Calcd.: C: 52.18; H: 8.58; N: 2.43. **Found:** C: 52.38; H: 8.45; N: 2.31. **IR** (ATR, cm^{-1}): 2096 (vs, $\nu_{C=N}$); 2043 (vs, $\nu_{C\equiv C}$); 1552 (s, $\nu_{C=C}$). **Raman** (cm^{-1}): 2101 (m, $\nu_{C=N}$); 2053 (vs, $\nu_{C\equiv C}$); 1556 (m, br, sh at 1575, $\nu_{C=C}$). **^{1}H NMR** (500 MHz, THF-d_8): δ = 5.93 (s, 3H, Ar-**H**), 2.35 - 2.24 (m, 12H, C**H**$_2$-CH$_3$), 1.96 - 1.88 (m, 24H, C**H**$_2$-CH$_3$), 1.86 - 1.77 (m, 36H, C**H**$_2$-CH$_3$ and C**H**$_2$-CH$_2$), 1.24 - 1.17 (m, 72H, CH$_2$-C**H**$_3$). **^{13}C{^{1}H} NMR** (125.8 MHz, THF-d_8): δ = 142.7 (s, Fe-N=**C**=S), 129.6 (s, Ar-**C**-C≡C), 127.5 (s, Ar-**C**-H), 123.8 (p, $^2J_{C-P}$ = 28.3 Hz, Fe-**C**≡C), 121.5 (s, Fe-C≡**C**), 21.5 - 21.3 (m, **C**H$_2$-**C**H$_2$), 20.7 - 20.4 (m, **C**H$_2$-CH$_3$), 9.6 (d, $^2J_{C-P}$ = 62.9 Hz, CH$_2$-**C**H$_3$). **^{31}P{^{1}H} NMR** (202.5 MHz, THF-d_8): δ = 74.6 (s).

NMR - Studies

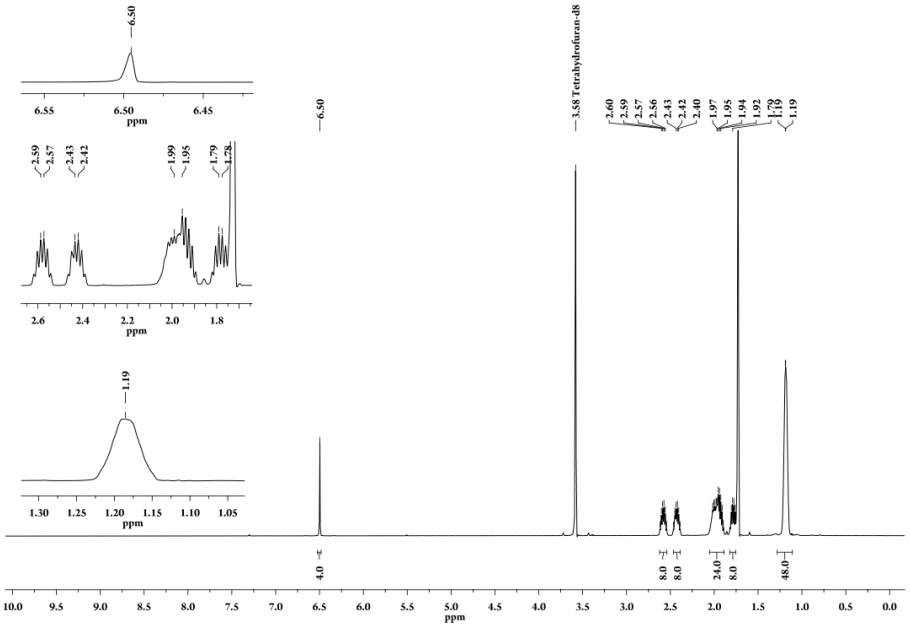

Figure S1. ^{1}H NMR of **1** in THF-d_8

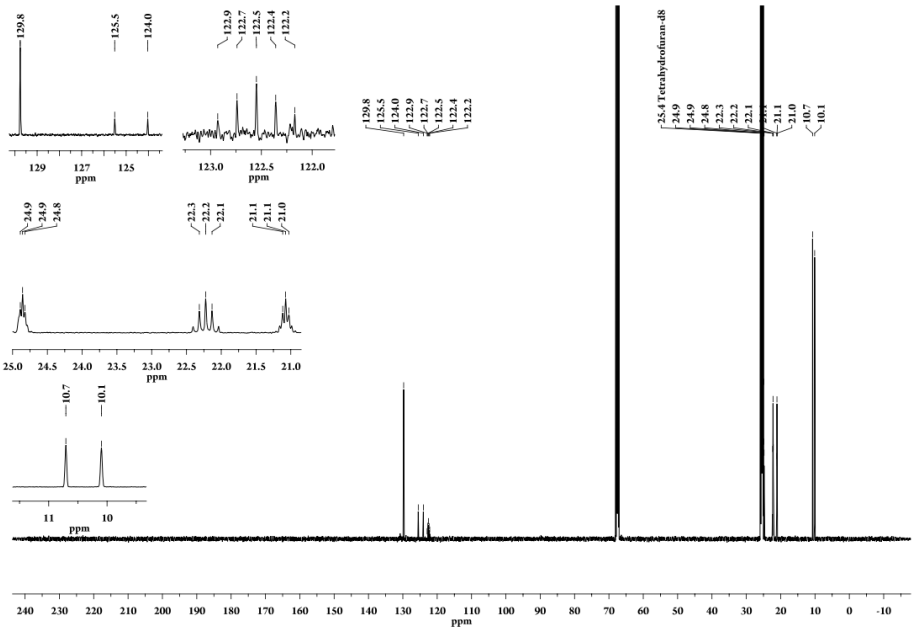

Figure S2. ^{13}C{^{1}H} NMR of **1** in THF-d_8

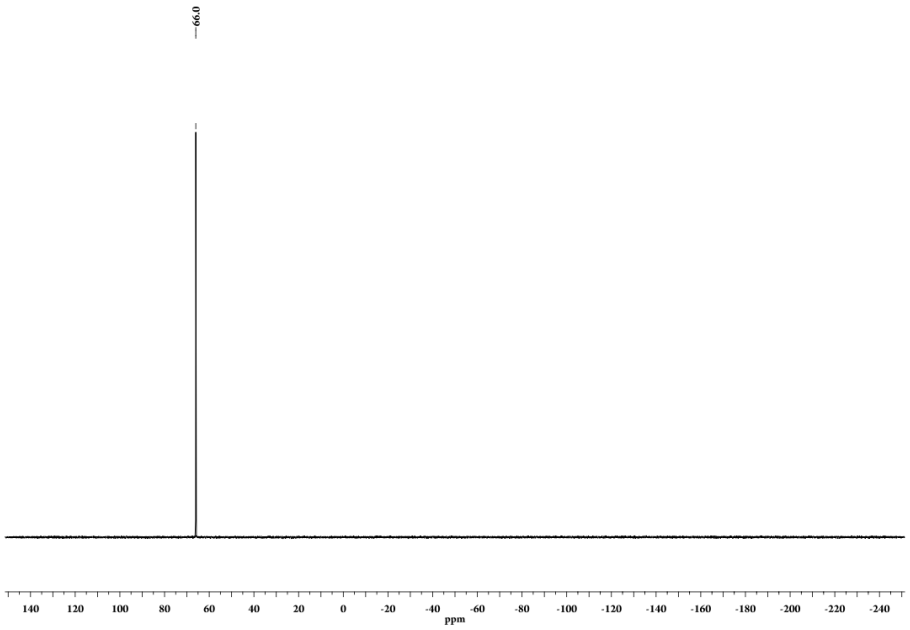

Figure S3. $^{31}P\{^{1}H\}$ NMR of **1** in THF-d_8

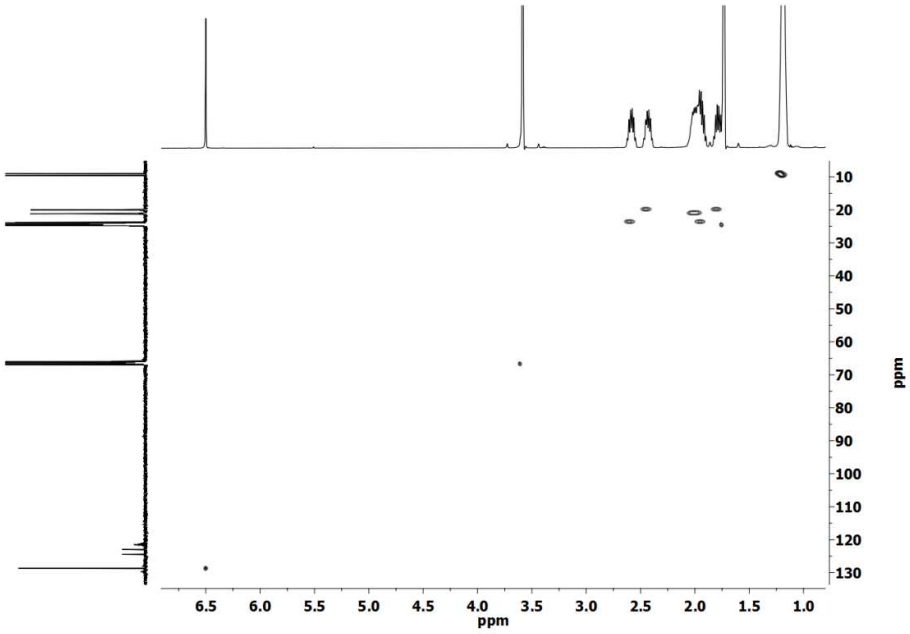

Figure S4. C,H Correlation NMR of **1** in THF-d_8

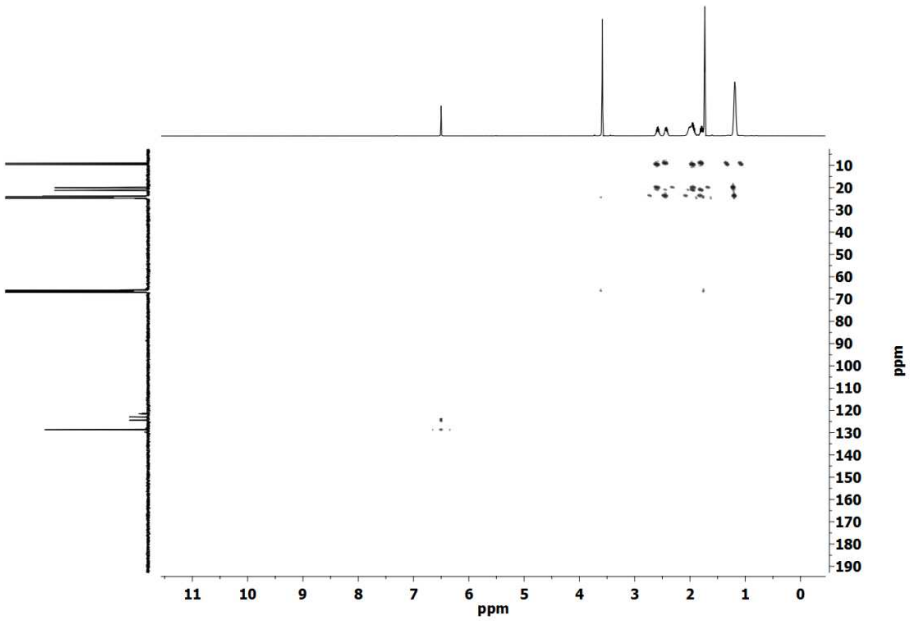

Figure S5. C,H Correlation (longrange) NMR of **1** in THF-d_8

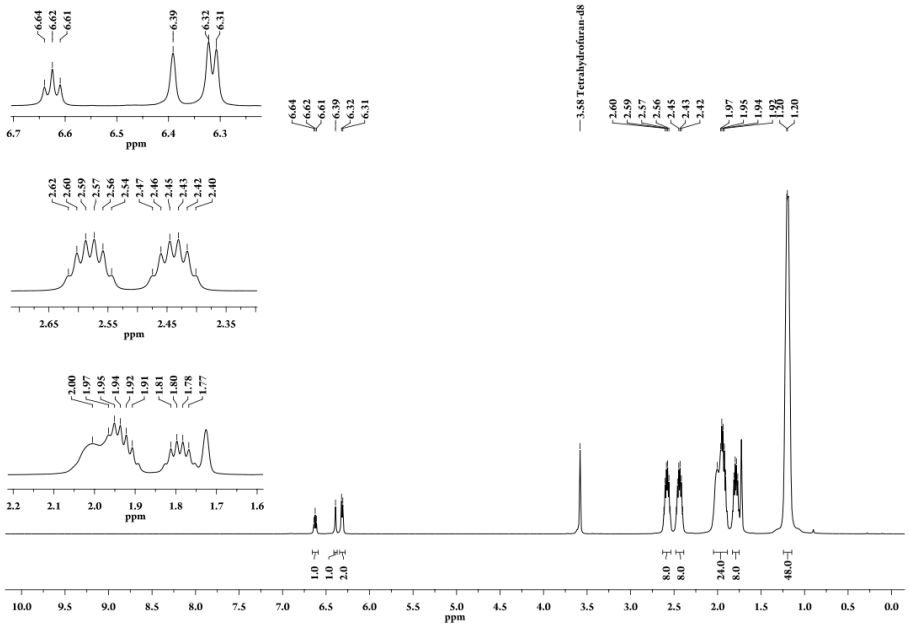

Figure S6. ^{1}H NMR of **2** in THF-d_8

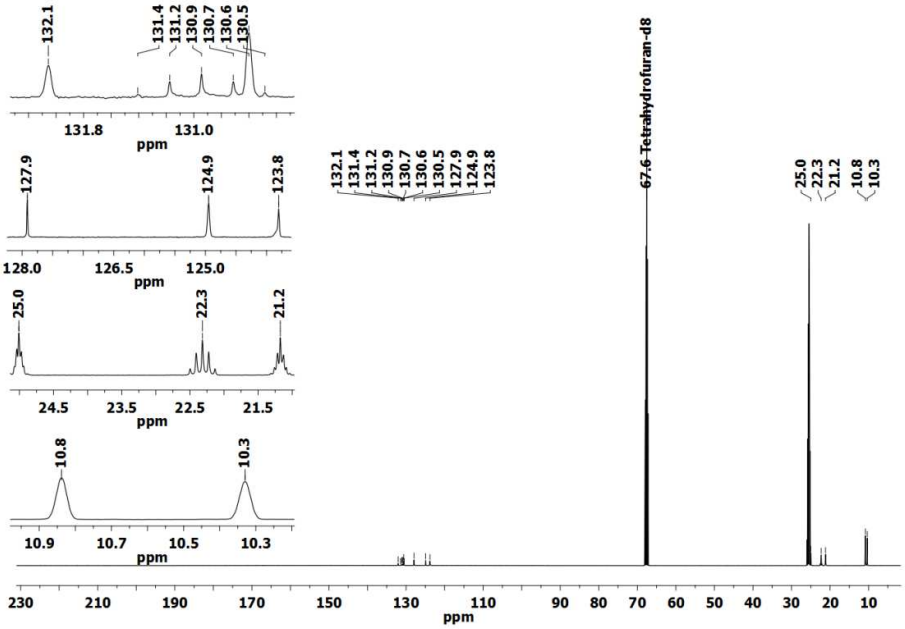

Figure S7. $^{13}C\{^{1}H\}$ NMR of **2** in THF-d_8

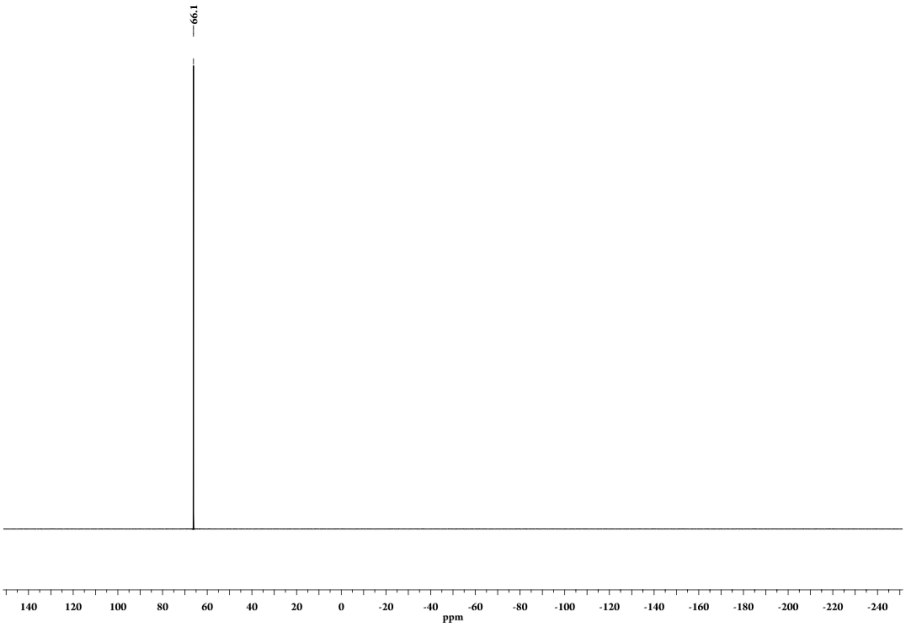

Figure S8. $^{31}P\{^{1}H\}$ NMR of **2** in THF-d_8

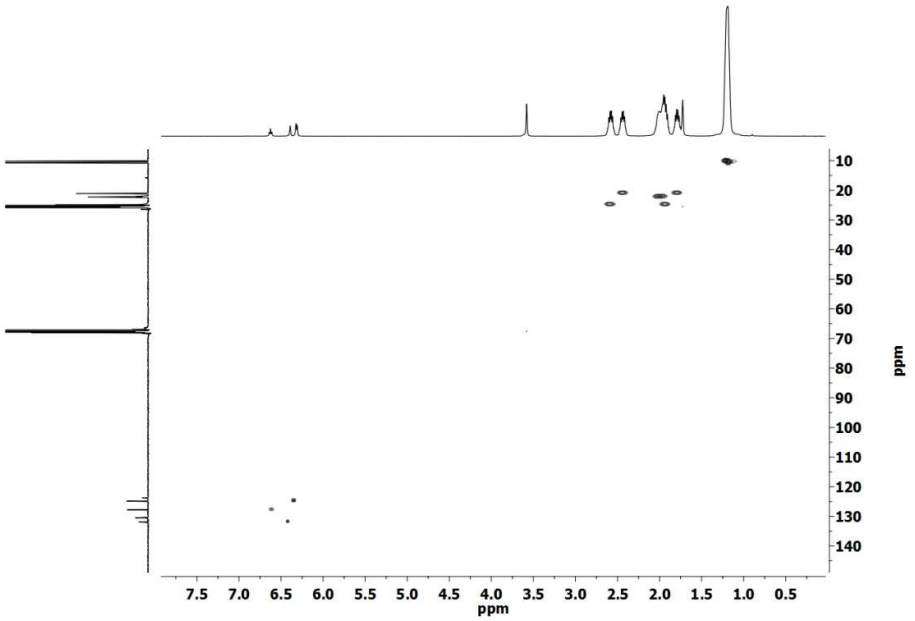

Figure S9. C,H Correlation NMR of **2** in THF-d_8

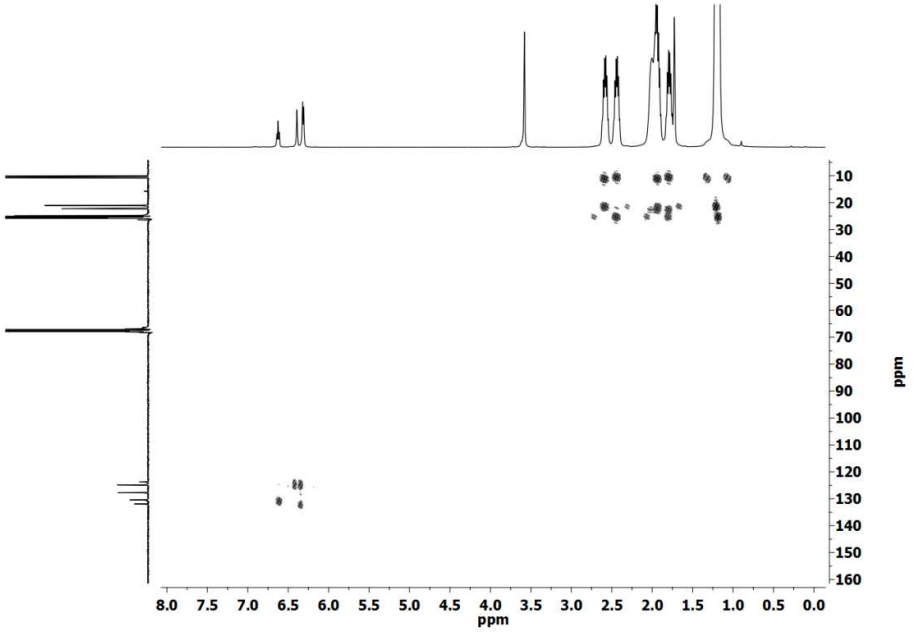

Figure S10. C,H Correlation (longrange) NMR of **2** in THF-d_8

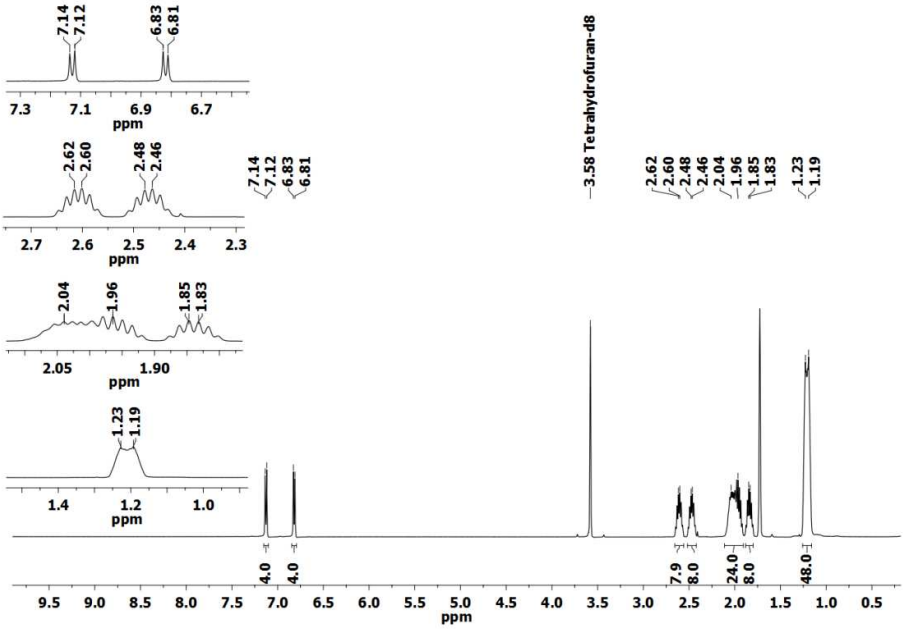

Figure S11. ^{1}H NMR of **3** in CD_2Cl_2

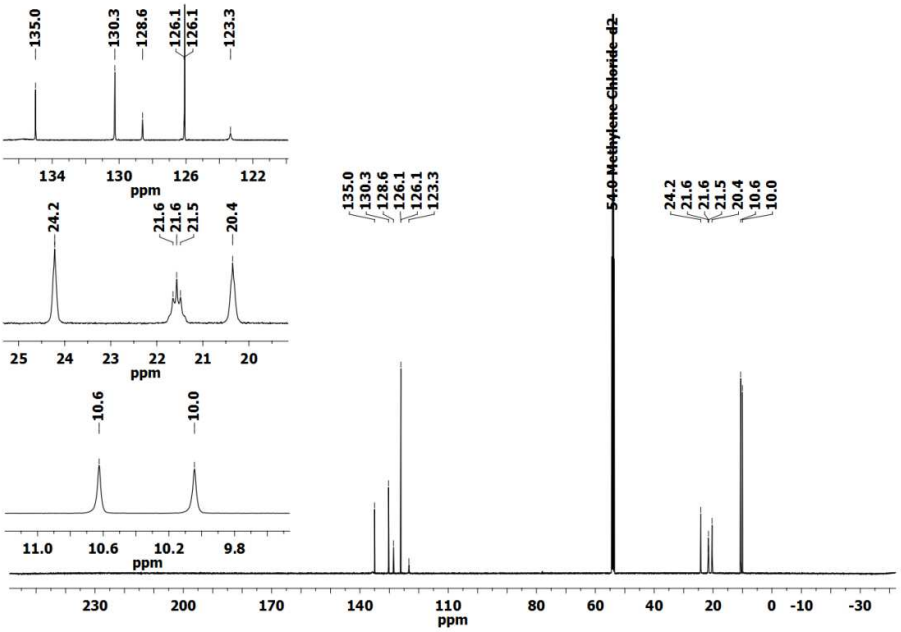

Figure S12. $^{13}C\{^{1}H\}$ NMR of **3** in CD_2Cl_2

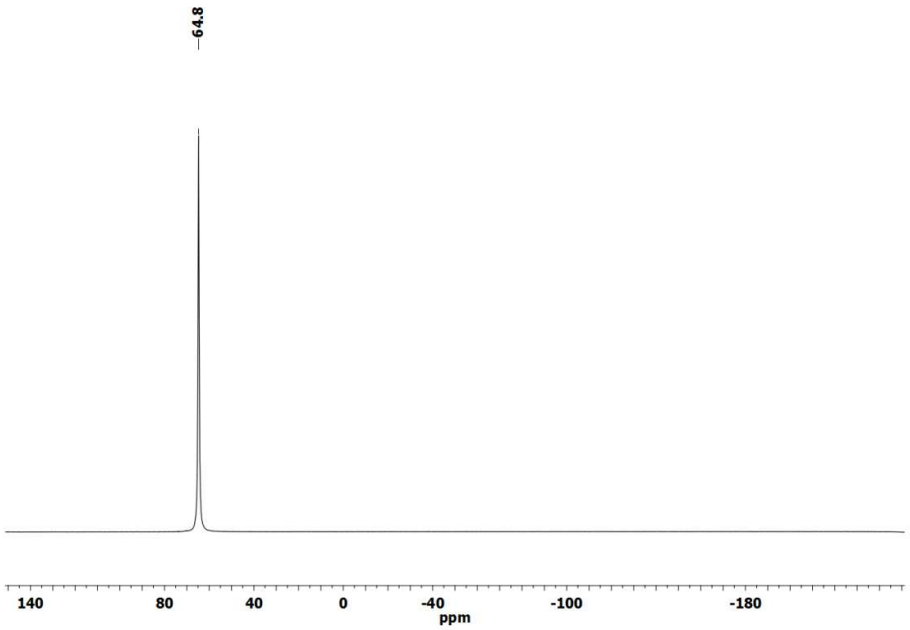

Figure S13. $^{31}P\{^{1}H\}$ NMR of **3** in CD_2Cl_2

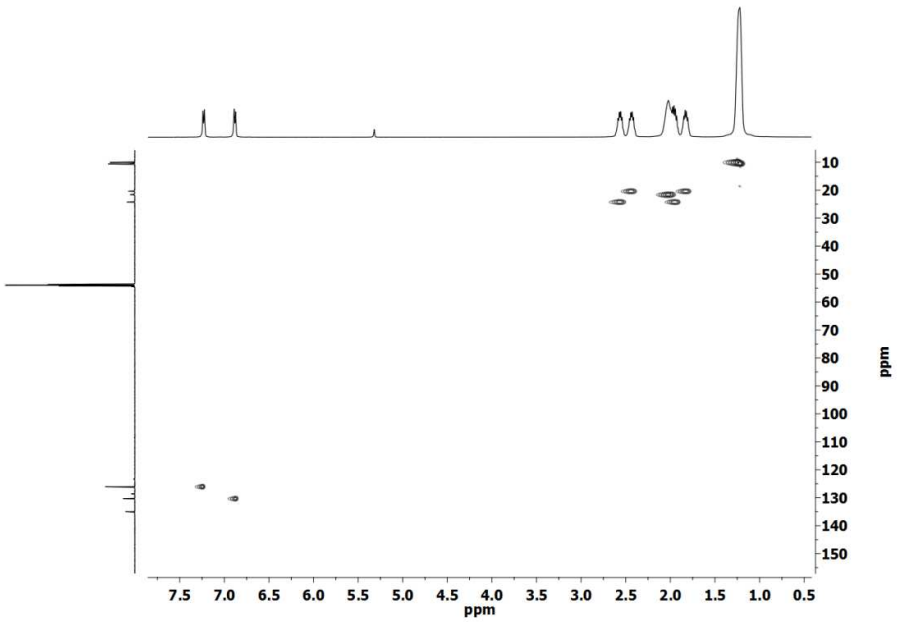

Figure S14. C,H Correlation of **3** in CD_2Cl_2

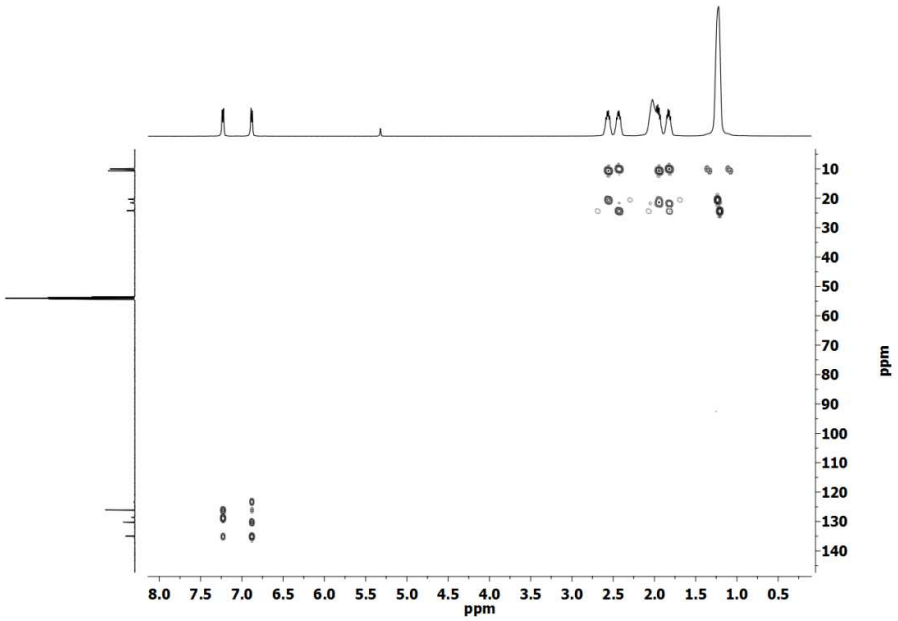

Figure S15. C,H Correlation (longrange) of **3** in CD_2Cl_2

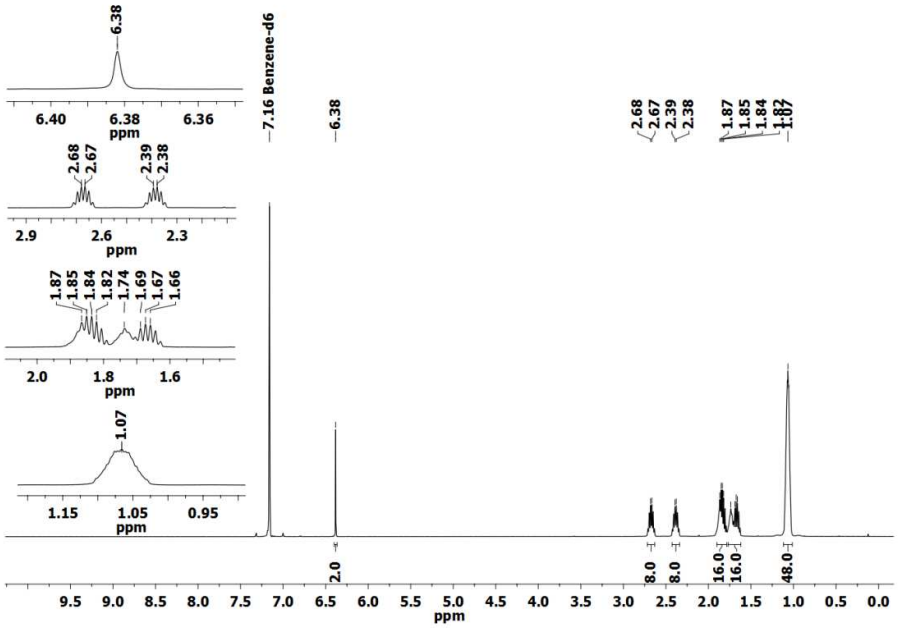

Figure S16. ^{1}H NMR of **4** in C_6D_6

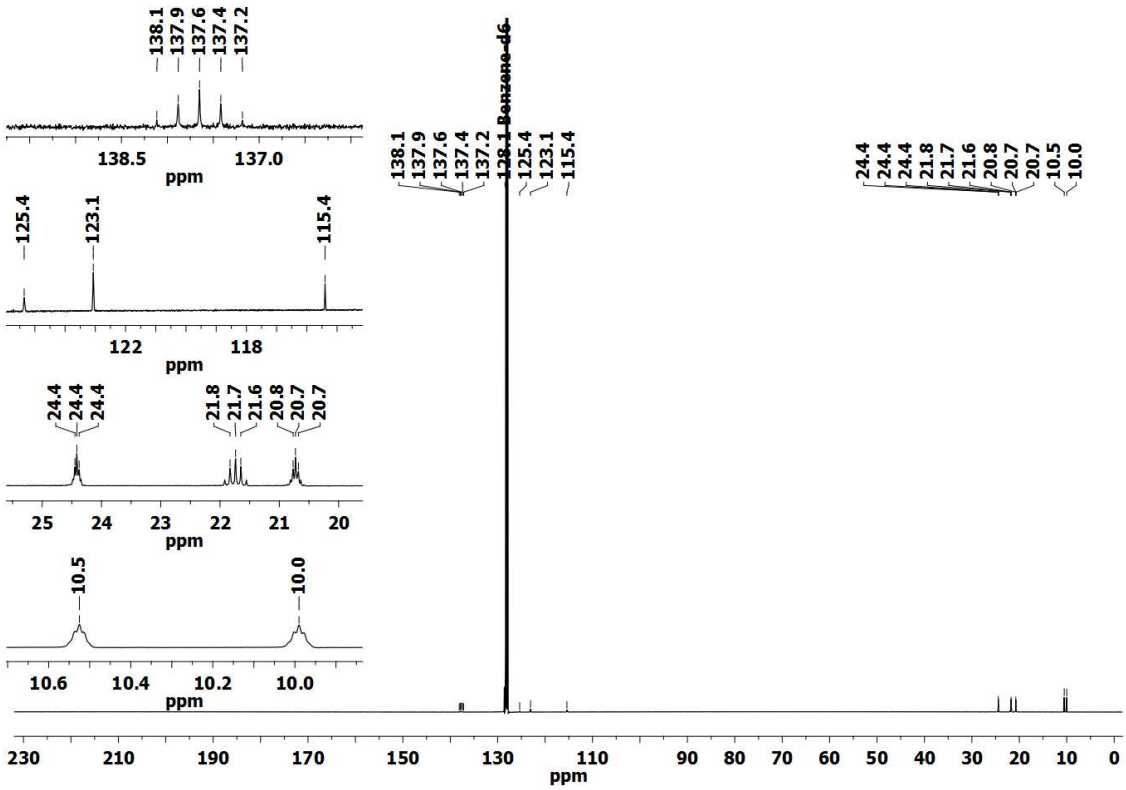

Figure S17. $^{13}C\{^1H\}$ NMR of **4** in C_6D_6

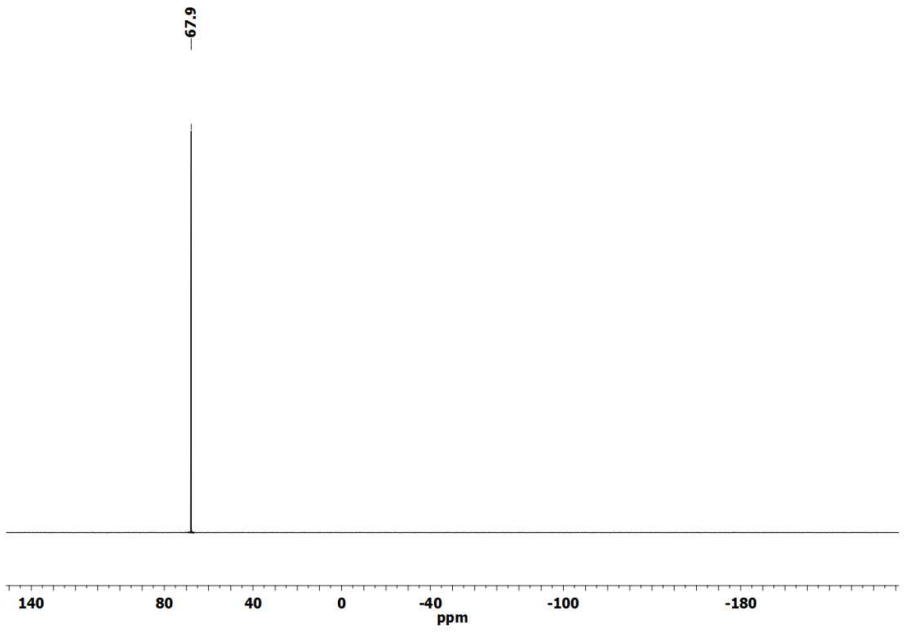

Figure S18. $^{31}P\{^1H\}$ NMR of **4** in C_6D_6

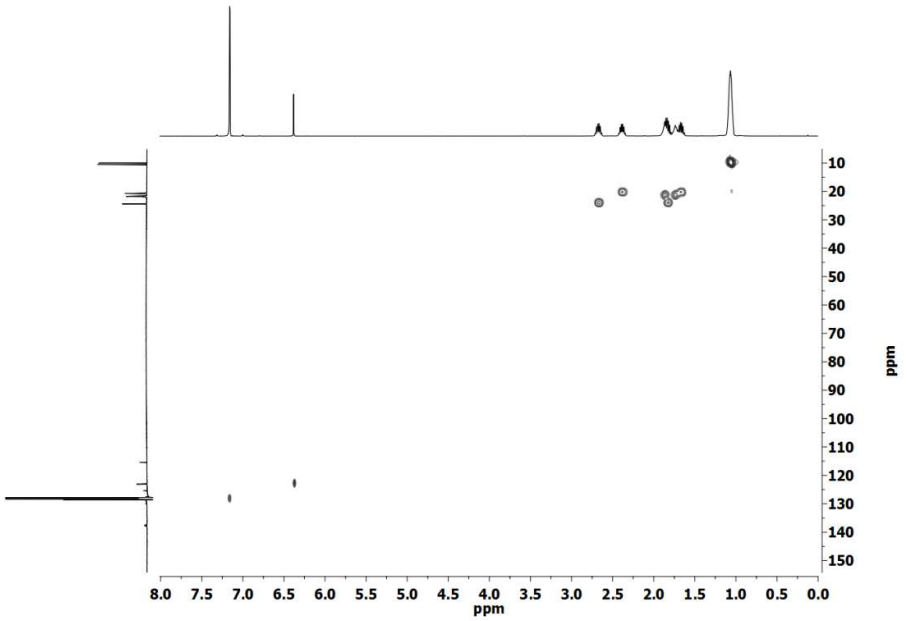

Figure S19. C,H-Correlation of **4** in C_6D_6

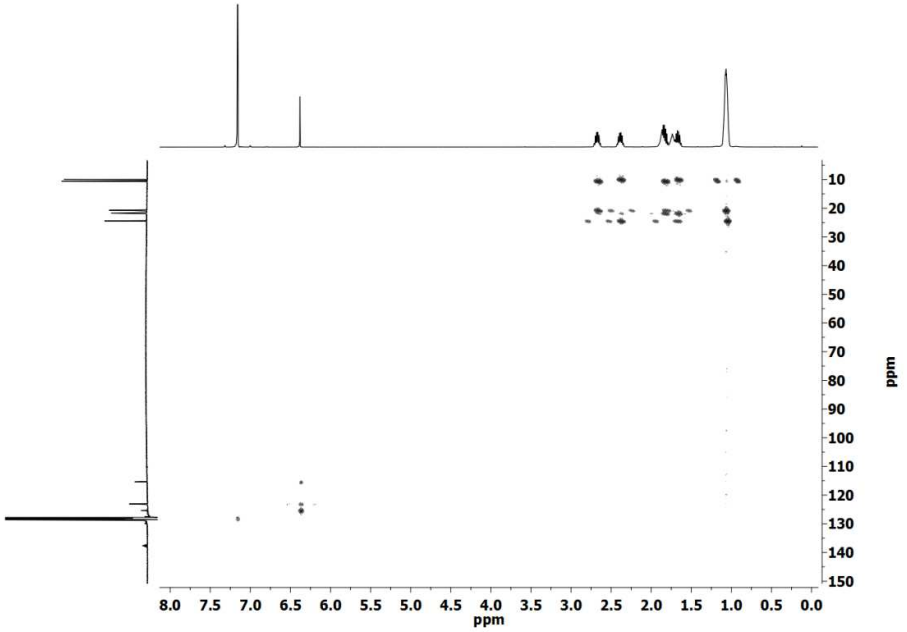

Figure S20. C,H-Correlation (longrange) of **4** in C_6D_6

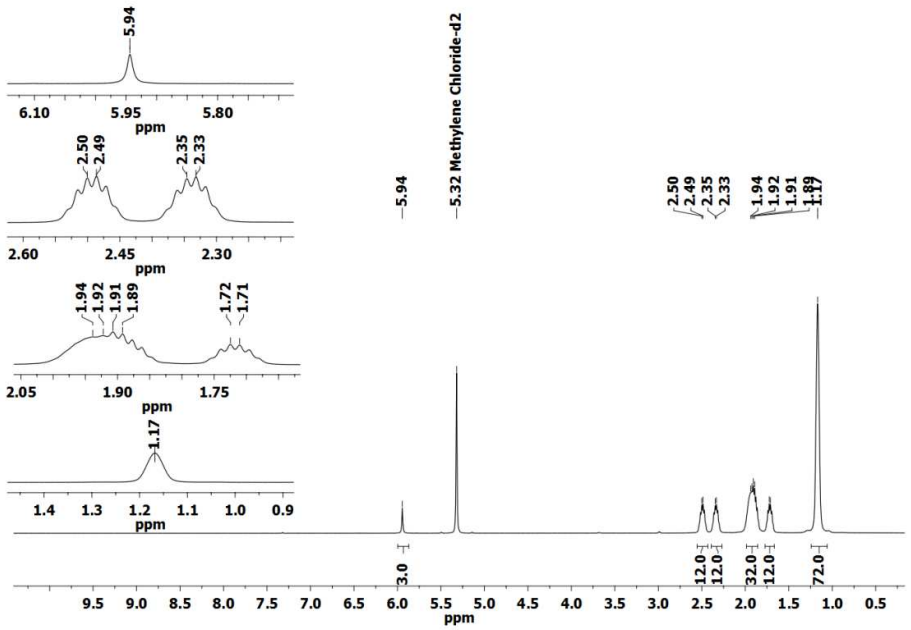

Figure S21. ^{1}H NMR of **5** in CD_2Cl_2

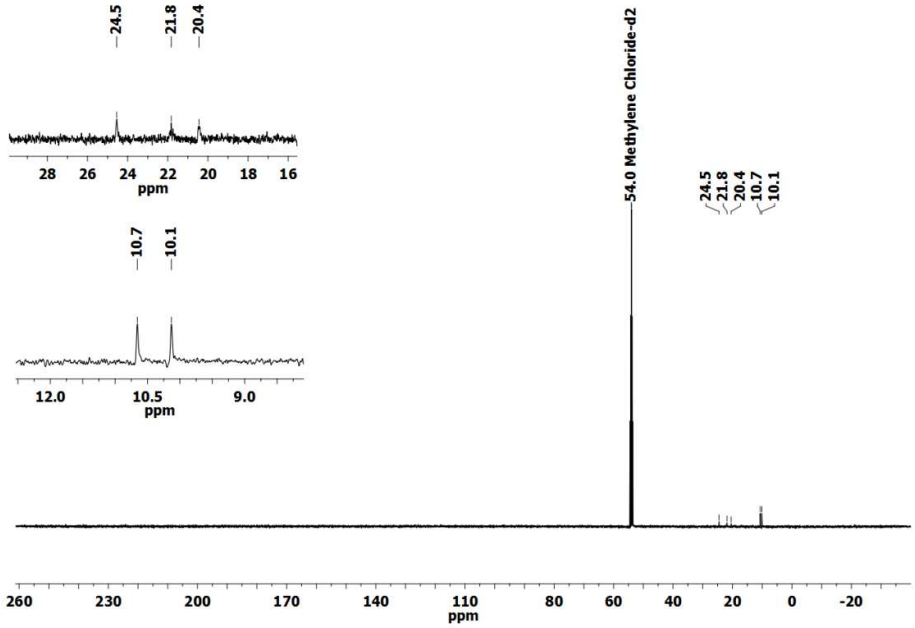

Figure S22. $^{13}C\{^{1}H\}$ NMR of **5** in CD_2Cl_2

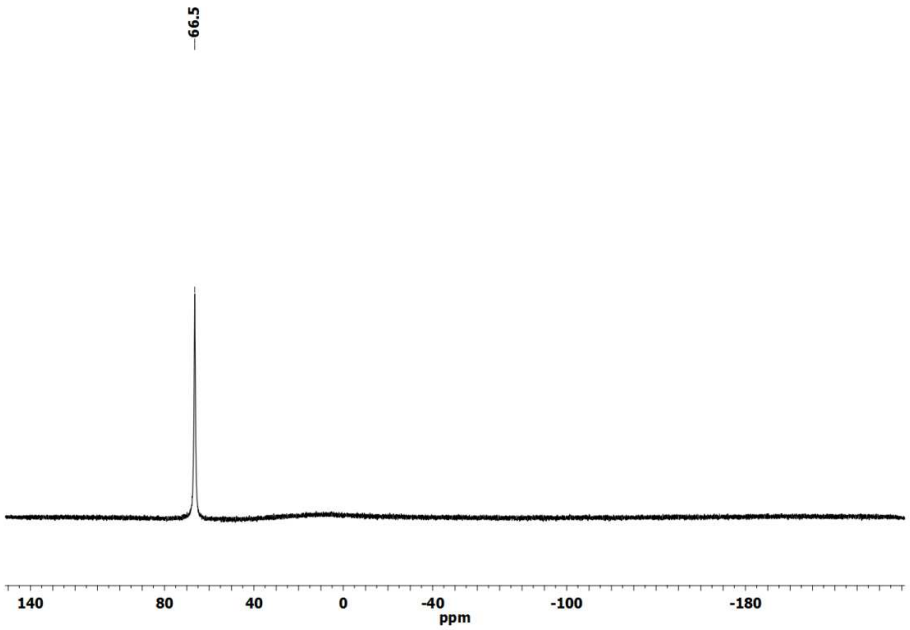

Figure S23. $^{31}P\{^{1}H\}$ NMR of **5** in CD_2Cl_2

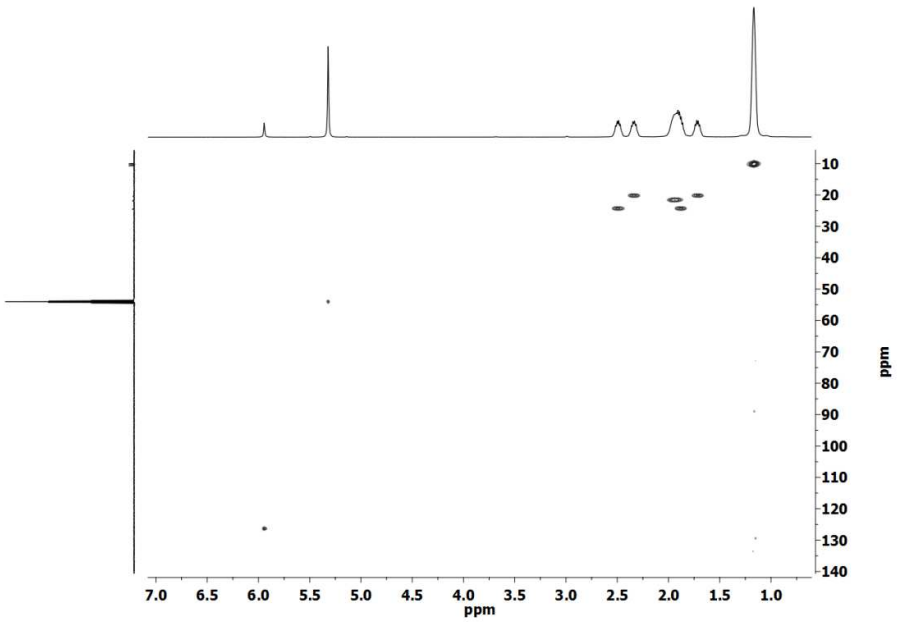

Figure S24. C,H Correlation of **5** in CD_2Cl_2

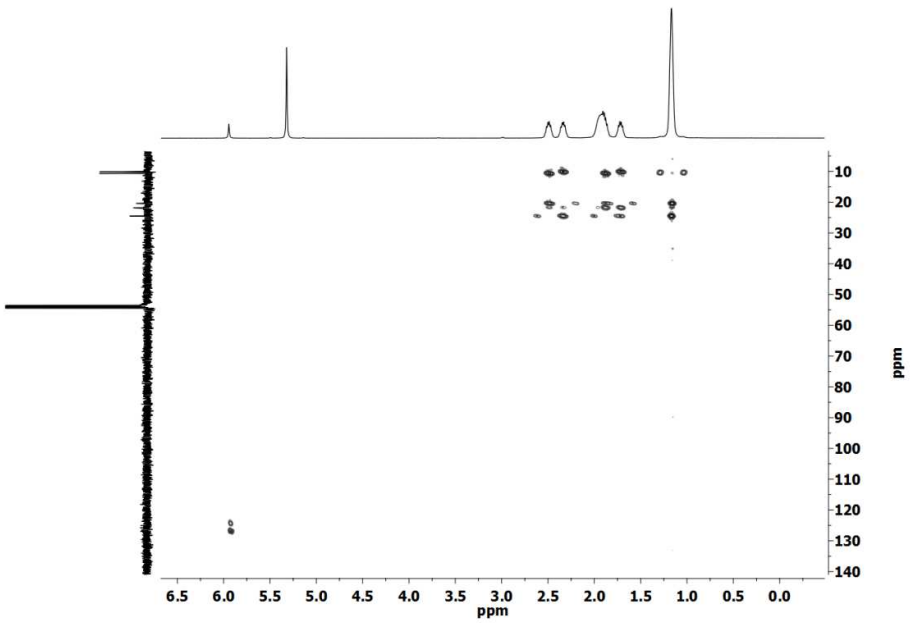

Figure S25. C,H Correlation (longrange) of **5** in CD_2Cl_2

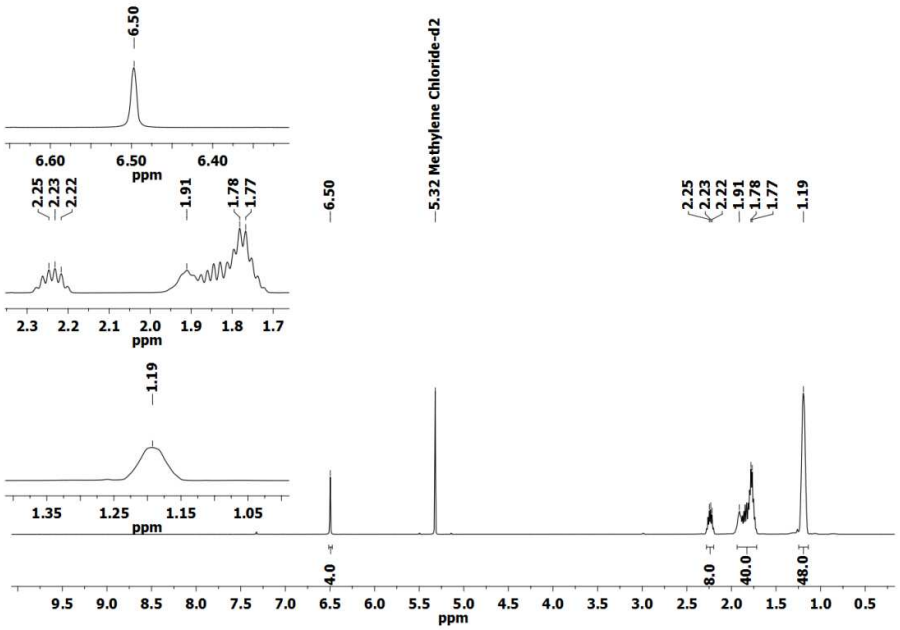

Figure S26. ^{1}H NMR of **6** in CD_2Cl_2

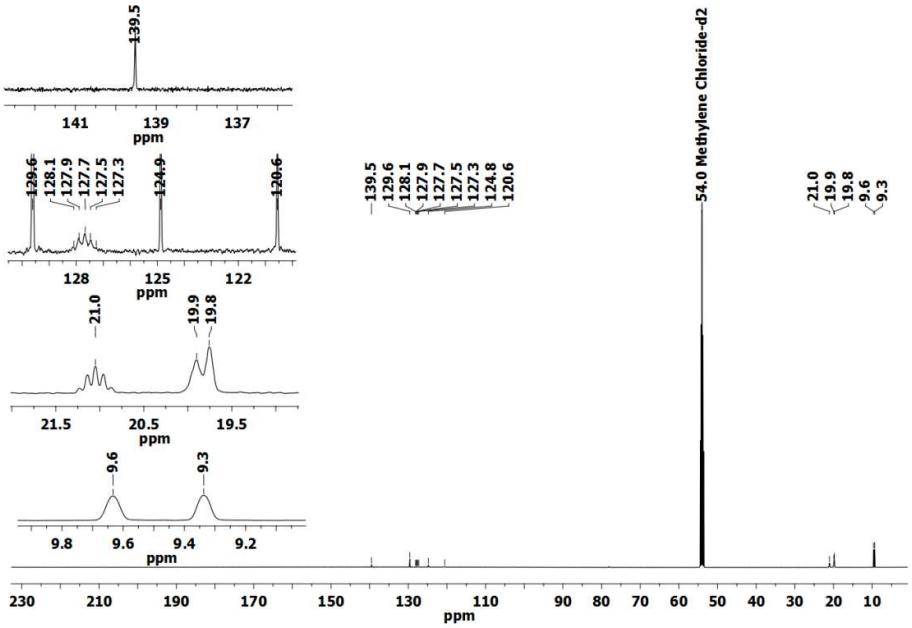

Figure S27. $^{13}C\{^{1}H\}$ NMR of **6** in CD_2Cl_2

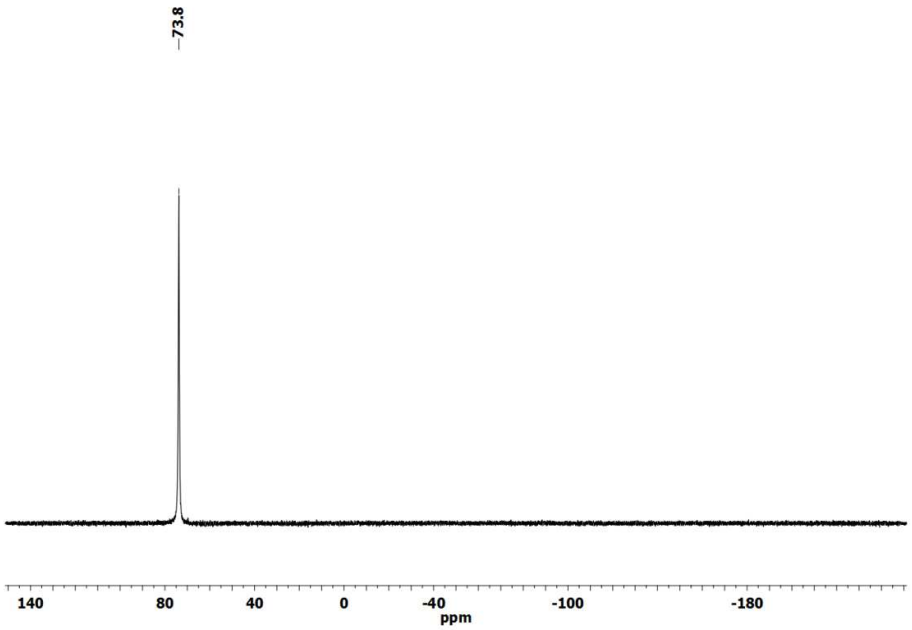

Figure S28. $^{31}P\{^{1}H\}$ NMR of **6** in CD_2Cl_2

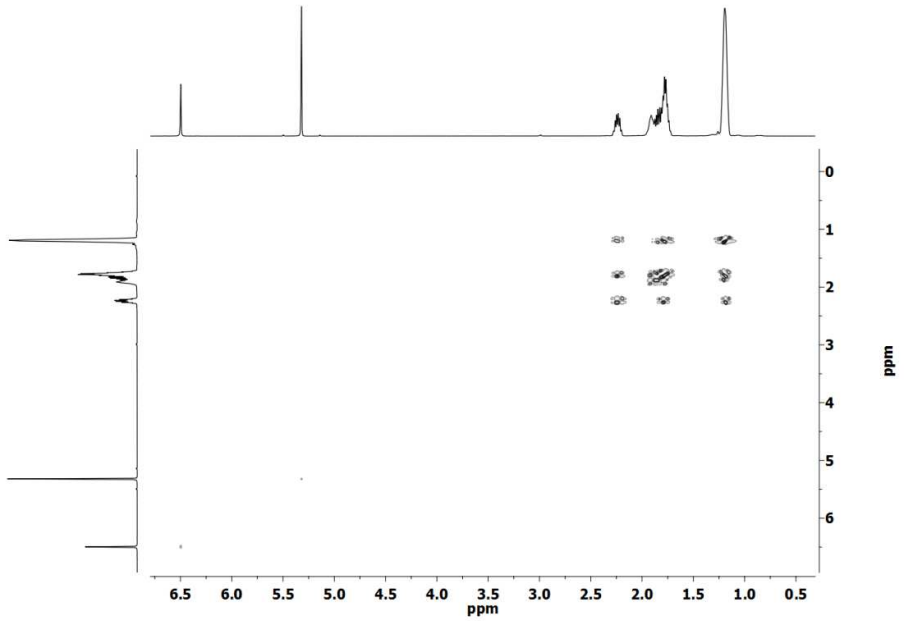

Figure S29. H,H Correlation (COSY) of **6** in CD_2Cl_2

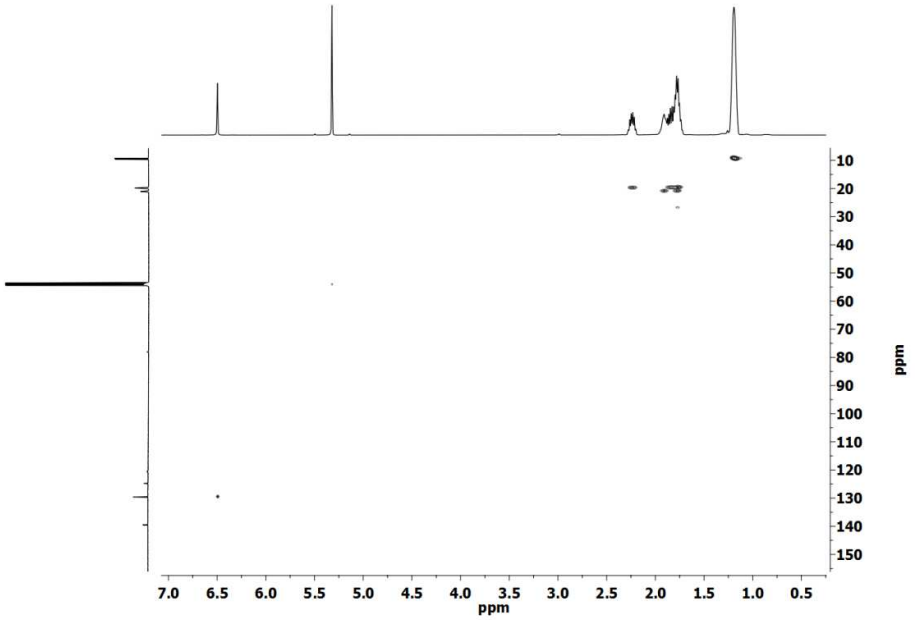

Figure S30. C,H Correlation of **6** in CD_2Cl_2

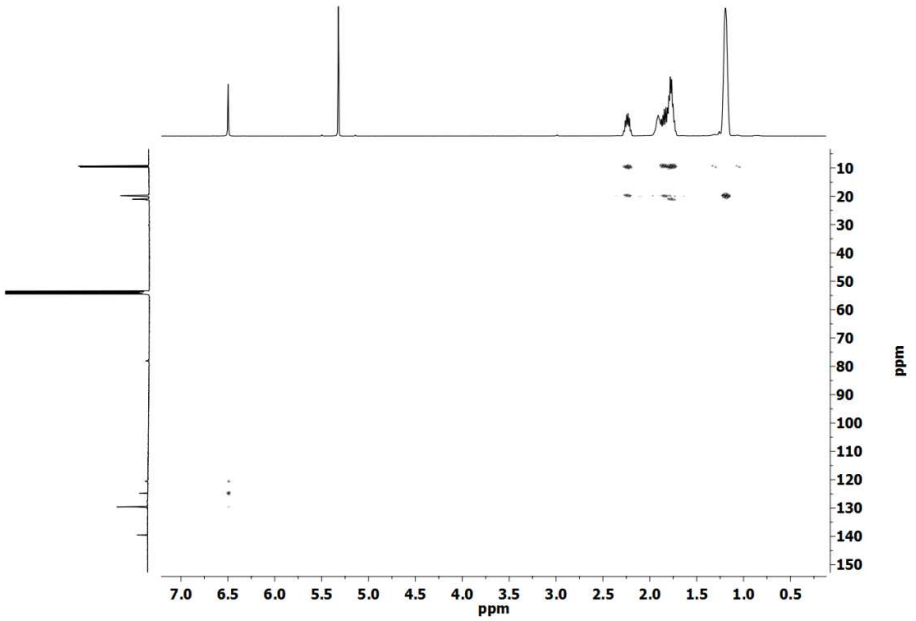

Figure S31. C,H Correlation (longrange) of **6** in CD_2Cl_2

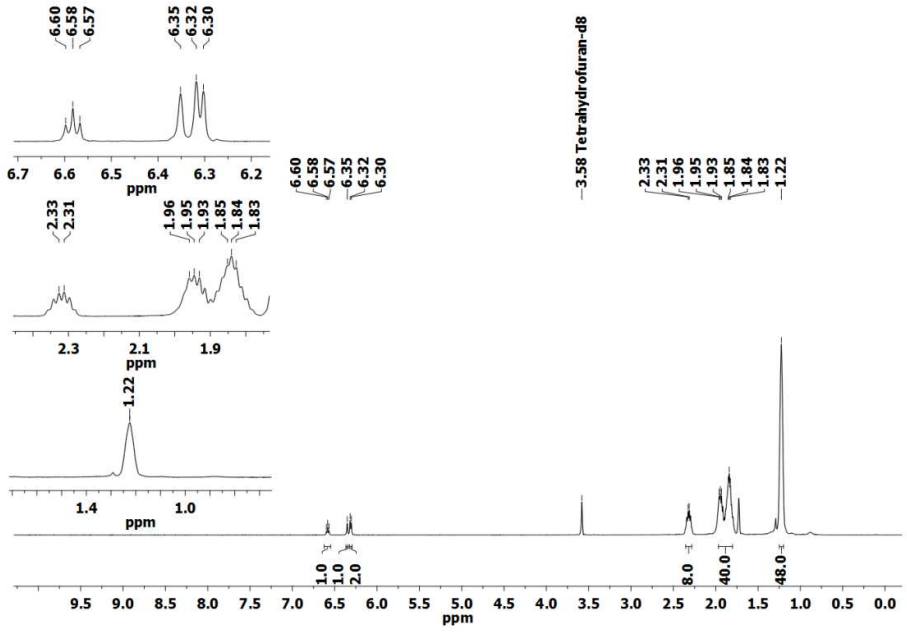

Figure S32. ^{1}H NMR of **7** in THF-d_8

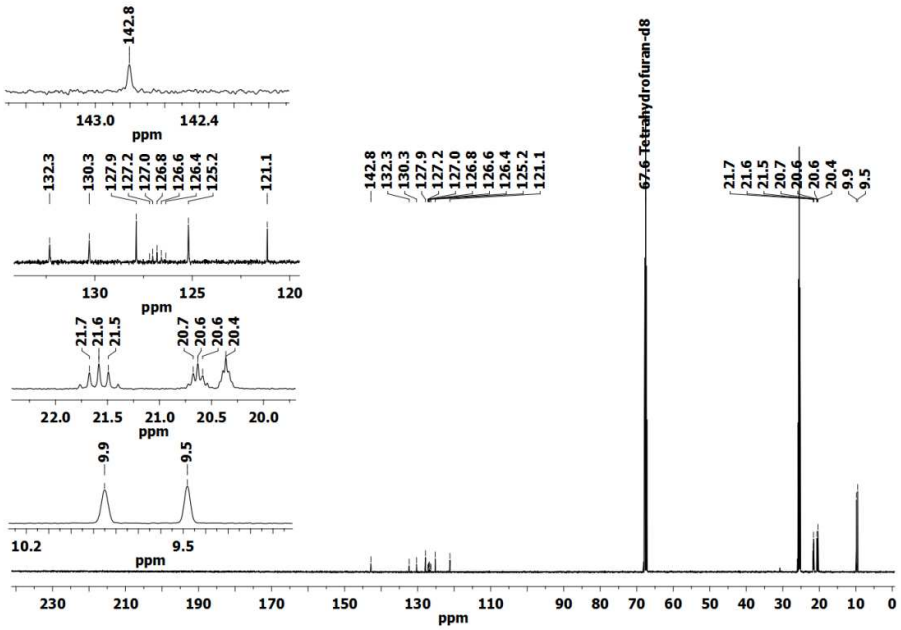

Figure S33. $^{13}C\{^{1}H\}$ NMR of **7** in THF-d_8

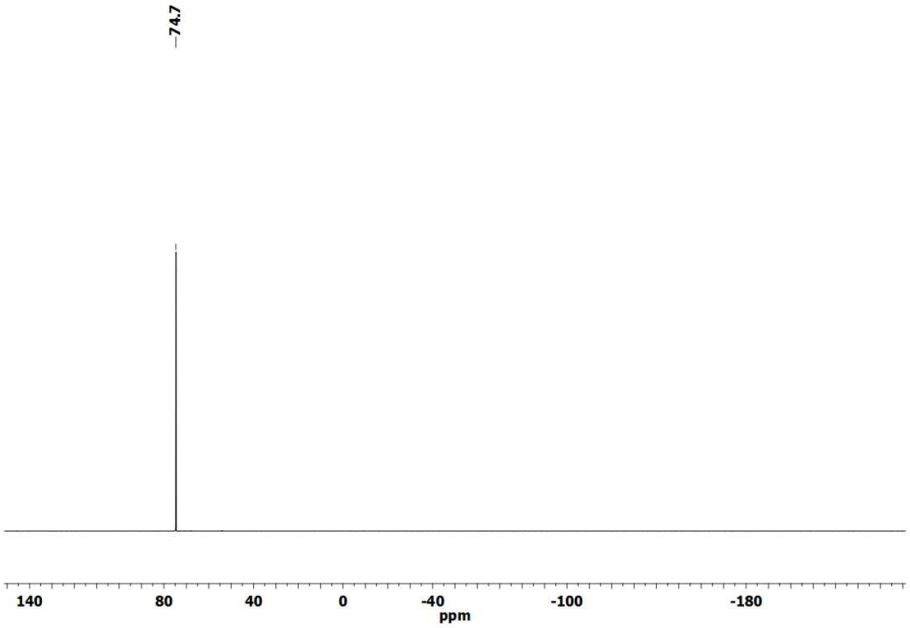

Figure S34. $^{31}P\{^{1}H\}$ NMR of **7** in THF-d_8

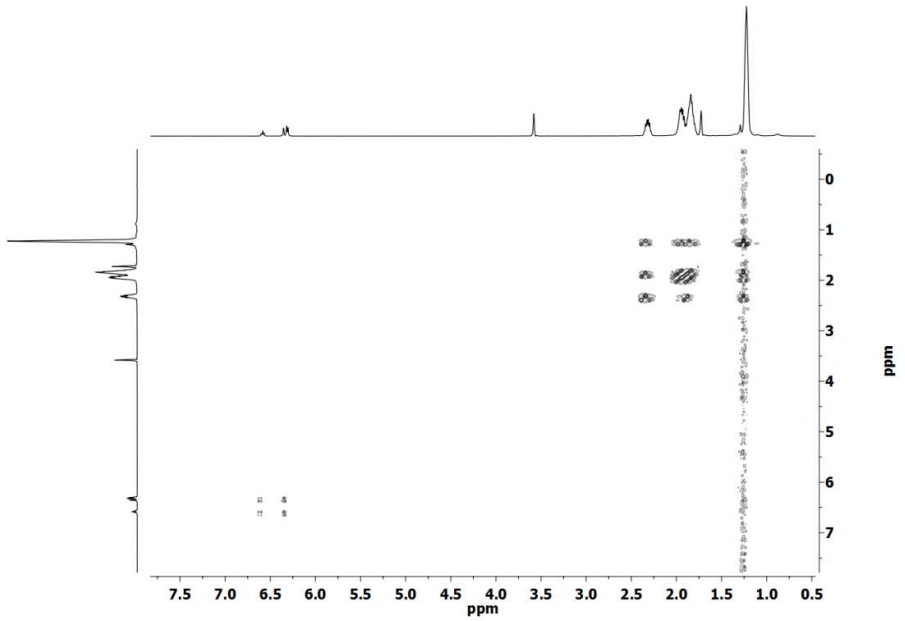

Figure S35. H,H Correlation (COSY) of **7** in THF-d_8

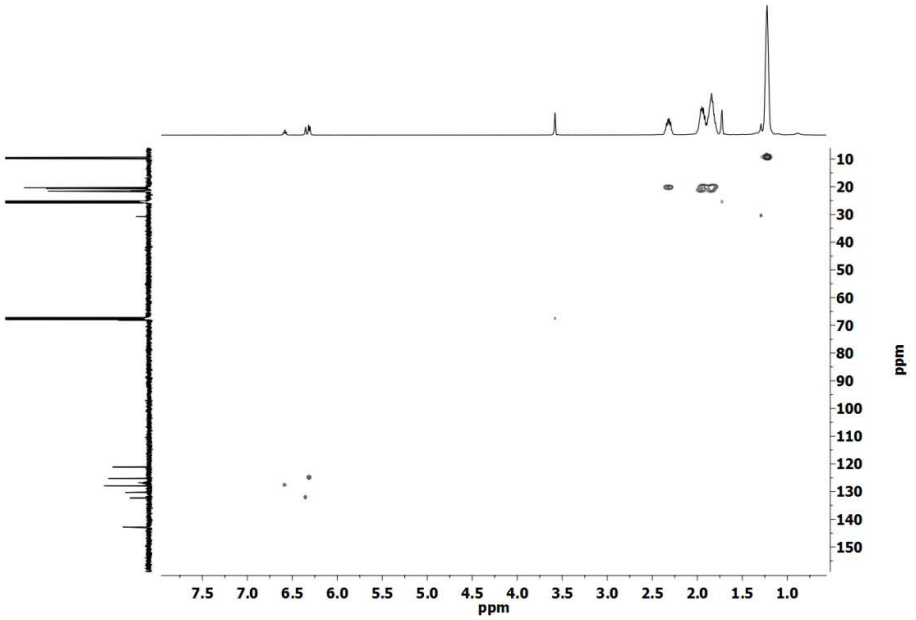

Figure S36. C, H Correlation of **7** in THF-d_8

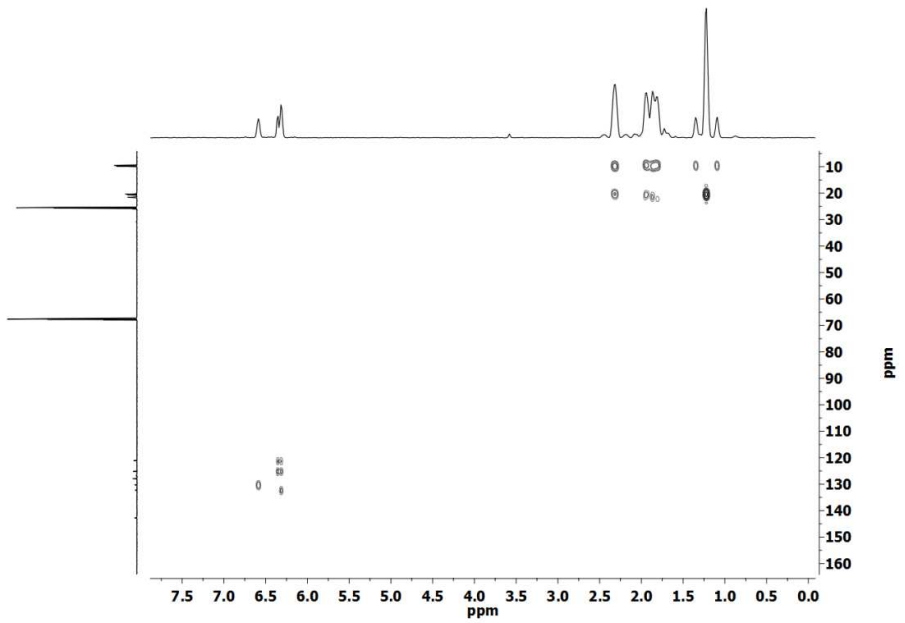

Figure S37. C, H Correlation (longrange) of **7** in THF-d_8

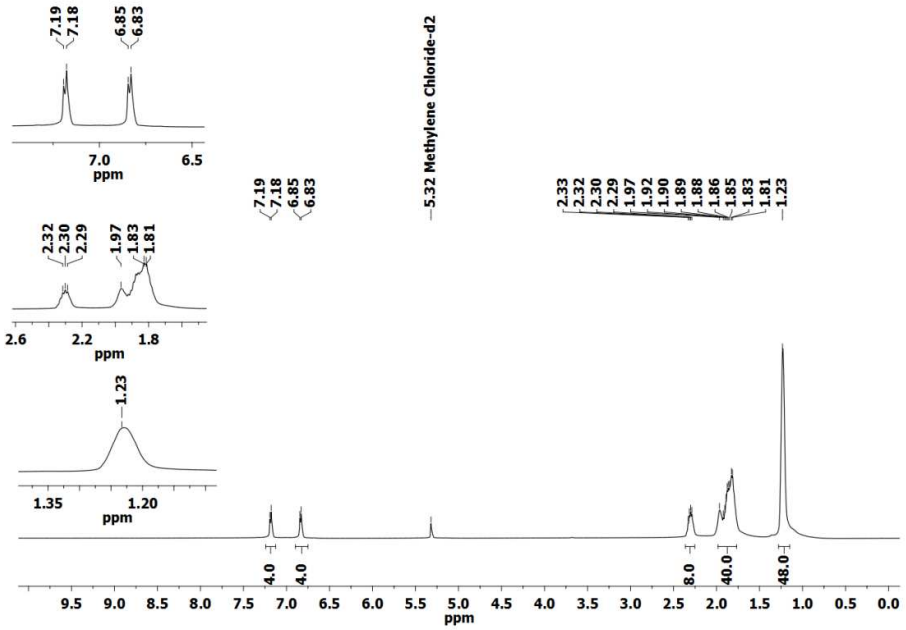

Figure S38. ^{1}H NMR of **8** in CD_2Cl_2

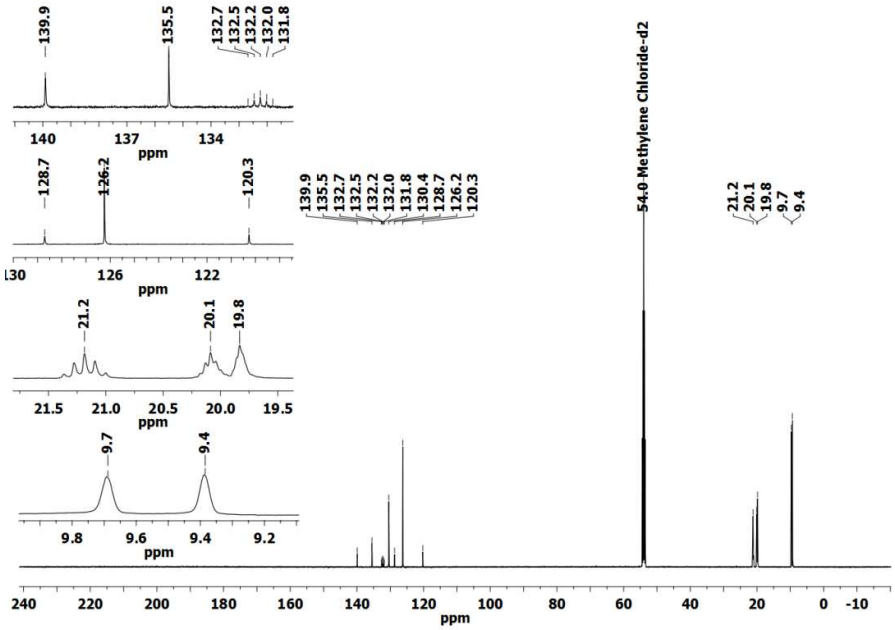

Figure S39. $^{13}C\{^{1}H\}$ NMR of **8** in CD_2Cl_2

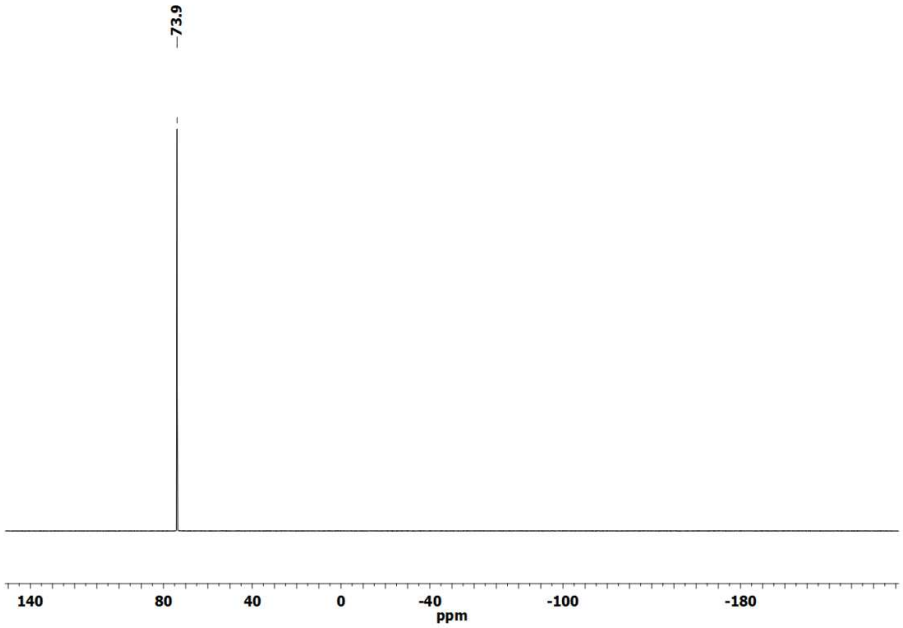

Figure S40. $^{31}P\{^{1}H\}$ NMR of **8** in CD_2Cl_2

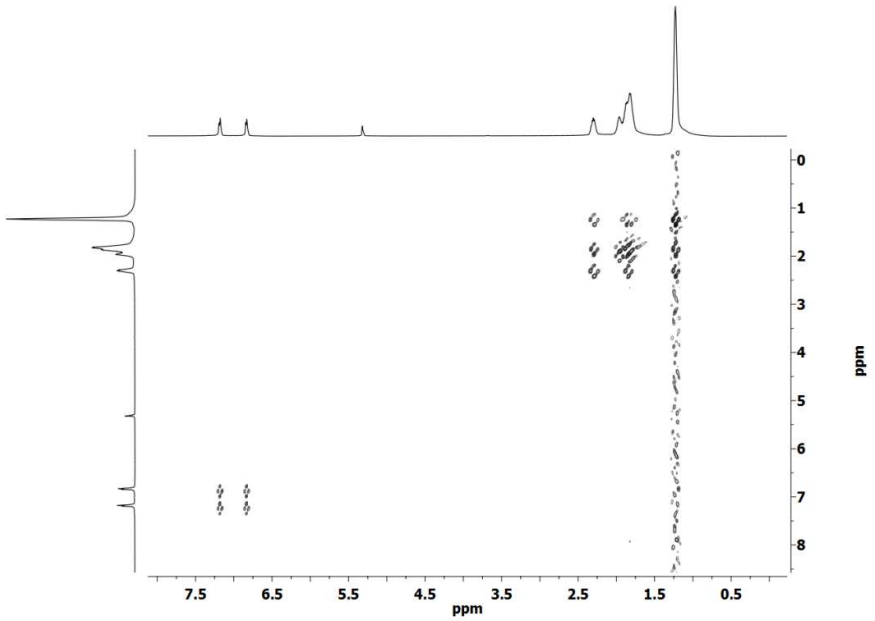

Figure S41. H,H Correlation (COSY) of **8** in CD_2Cl_2

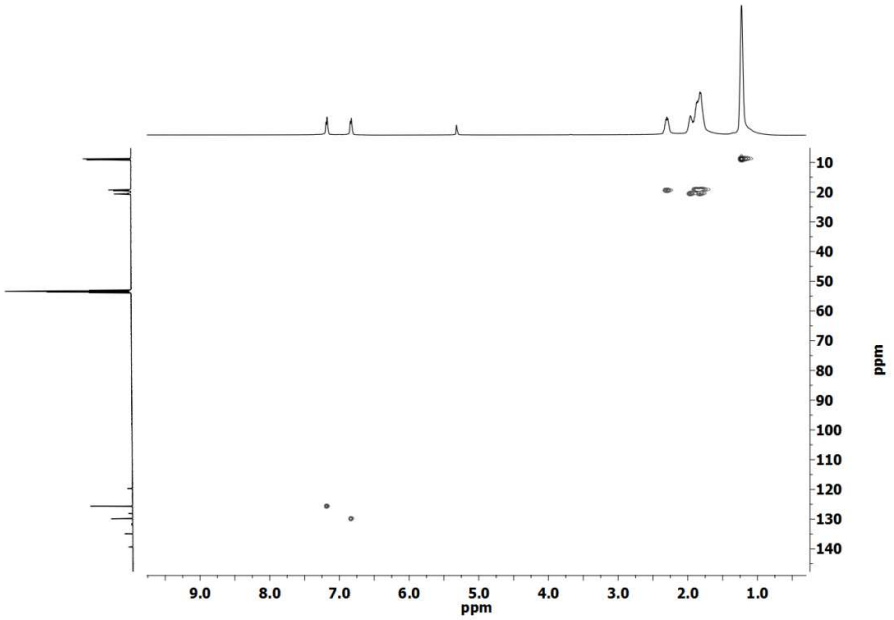

Figure S42. C,H Correlation of **8** in CD_2Cl_2

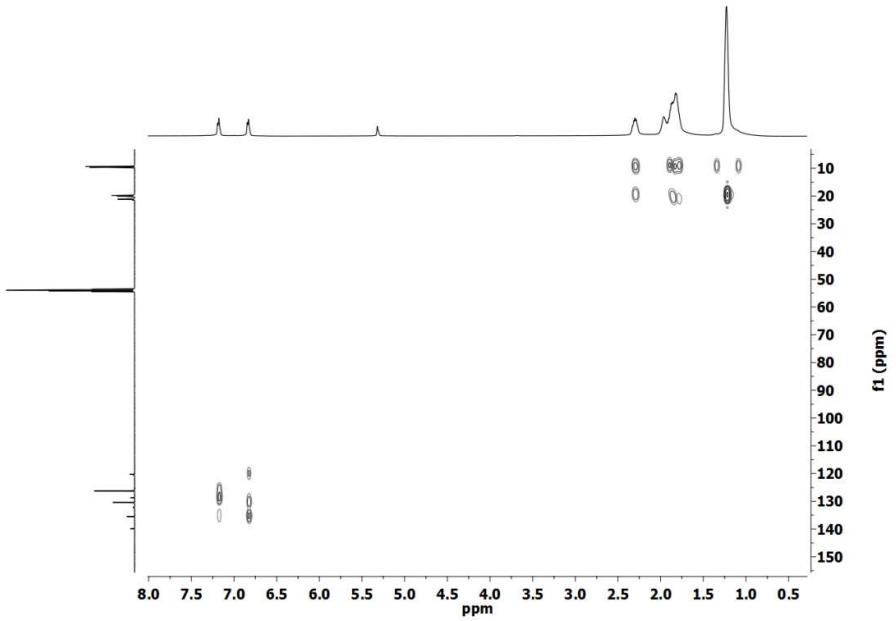

Figure S43. C,H Correlation (longrange) of **8** in CD_2Cl_2

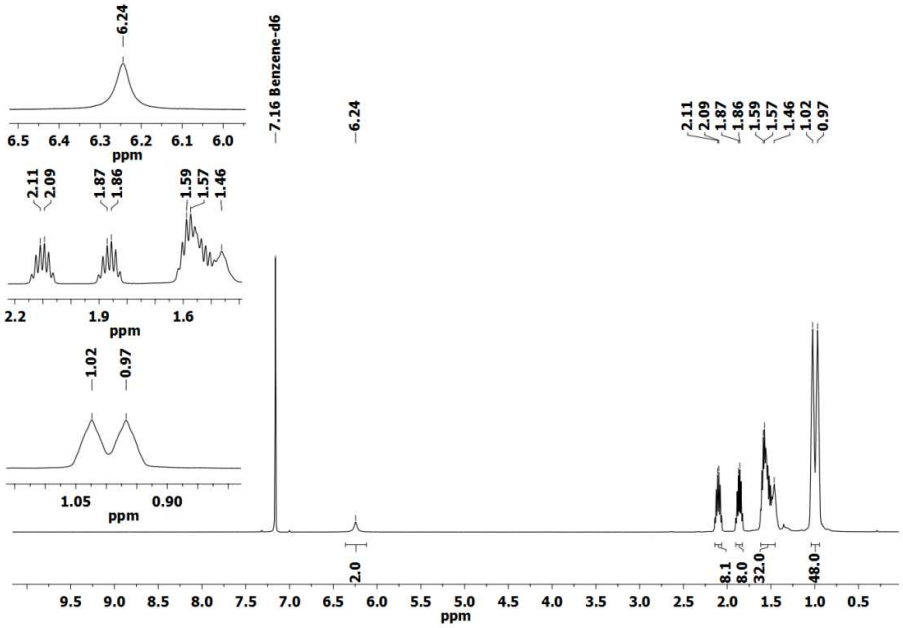

Figure S44. ^{1}H NMR of **9** in C_6D_6

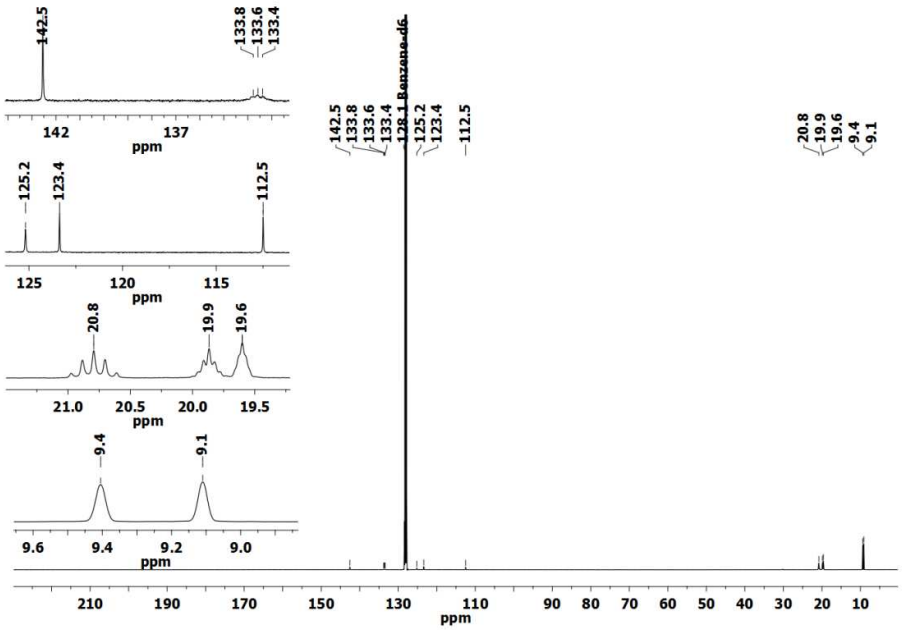

Figure S45. $^{13}C\{^1H\}$ NMR of **9** in C_6D_6

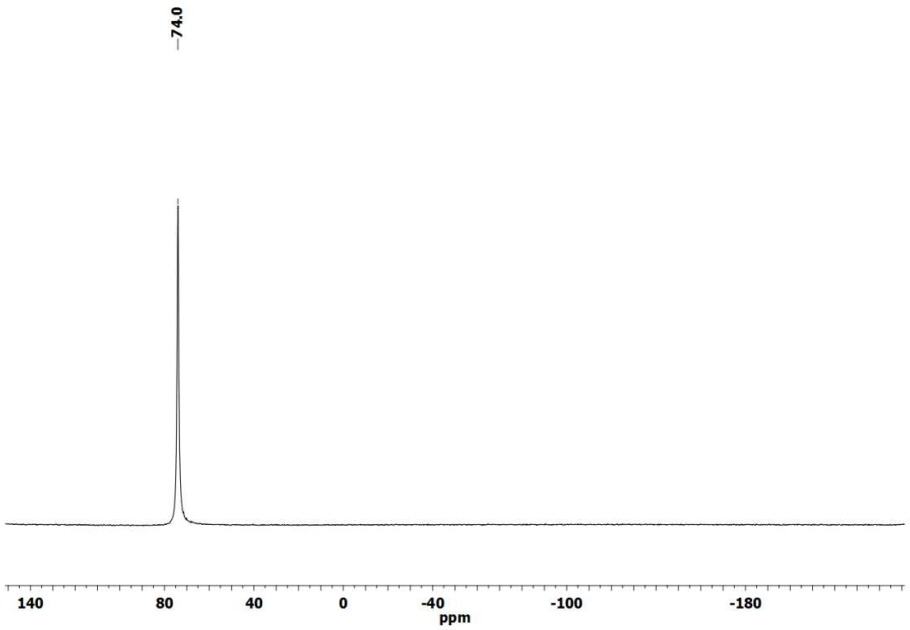

Figure S46. $^{31}P\{^1H\}$ NMR of **9** in C_6D_6

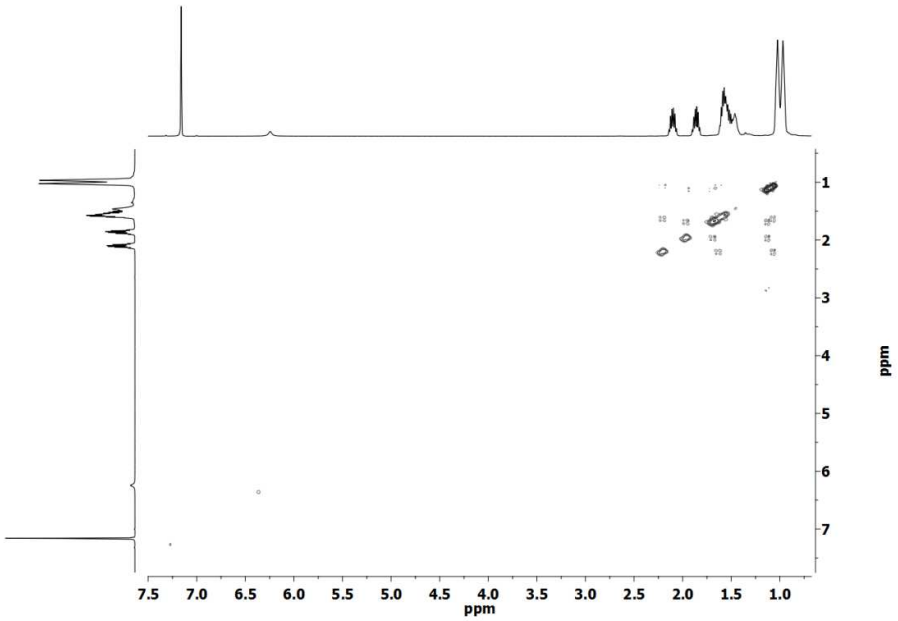

Figure S47. H,H Correlation (COSY) of **9** in C_6D_6

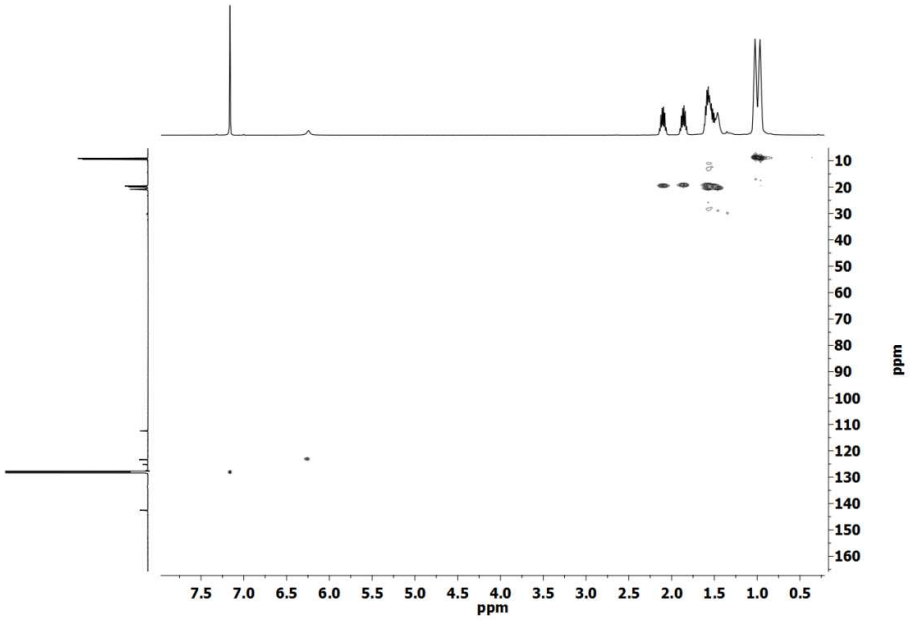

Figure S48. C,H Correlation of **9** in C_6D_6

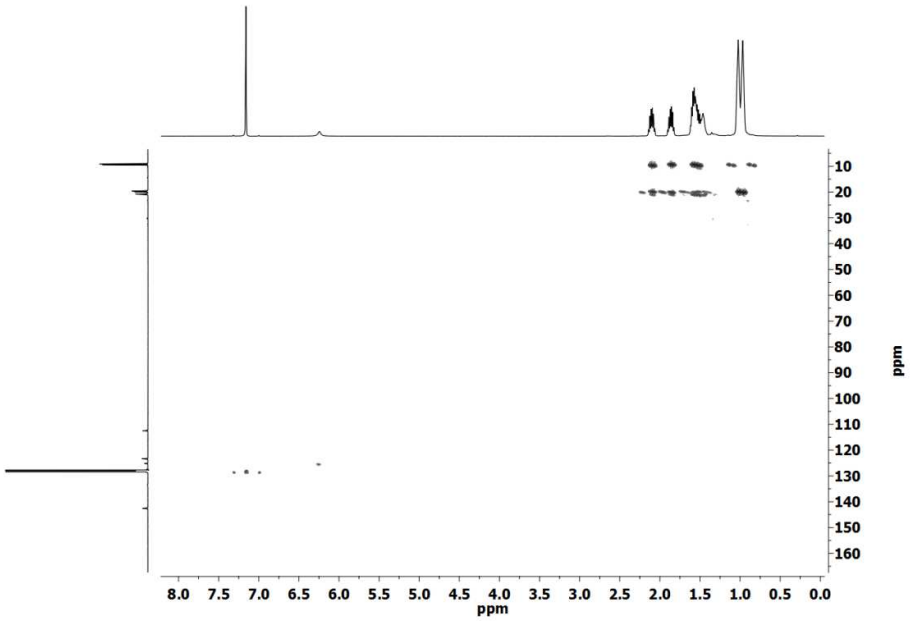

Figure S49. C,H Correlation (longrange) of **9** in C_6D_6

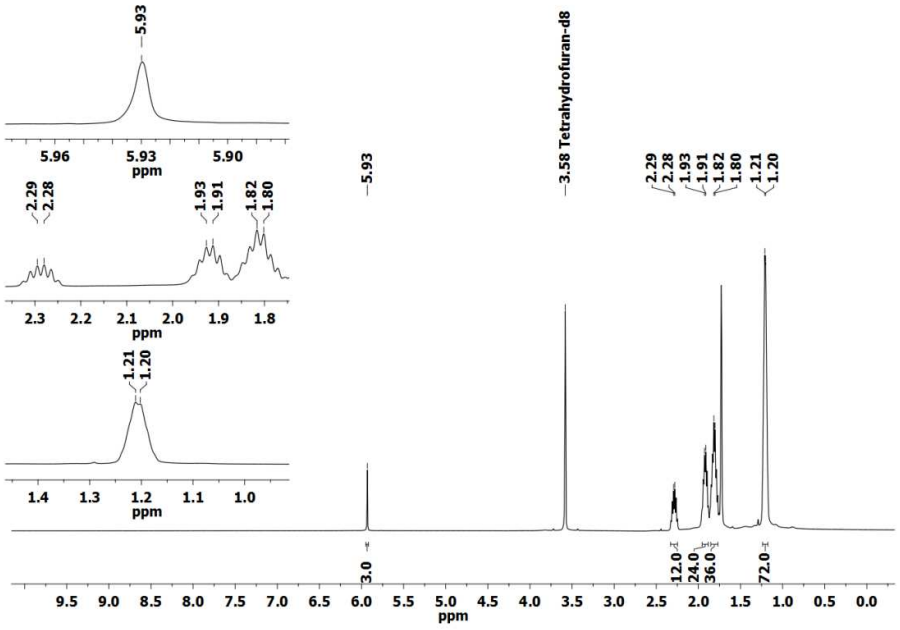

Figure S50. ^{1}H NMR of **10** in THF-d_8

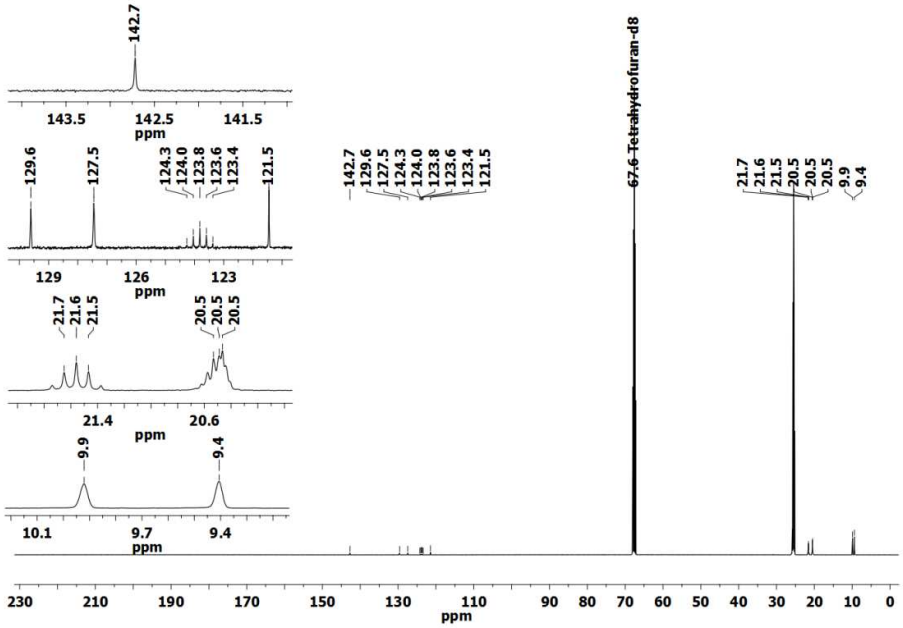

Figure S51. $^{13}C\{^{1}H\}$ NMR of **10** in THF-d_8

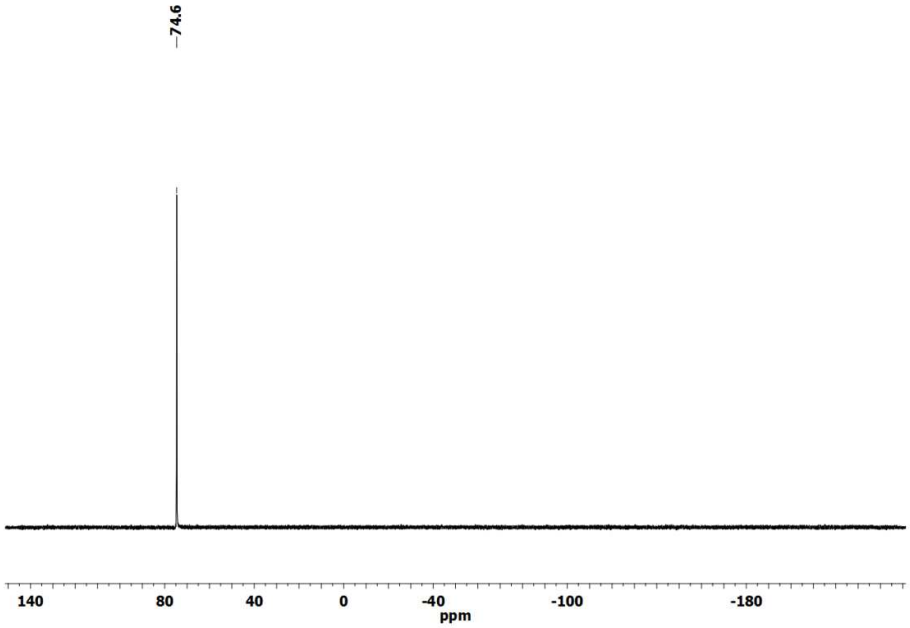

Figure S52. $^{31}P\{^{1}H\}$ NMR of **10** in THF-d_8

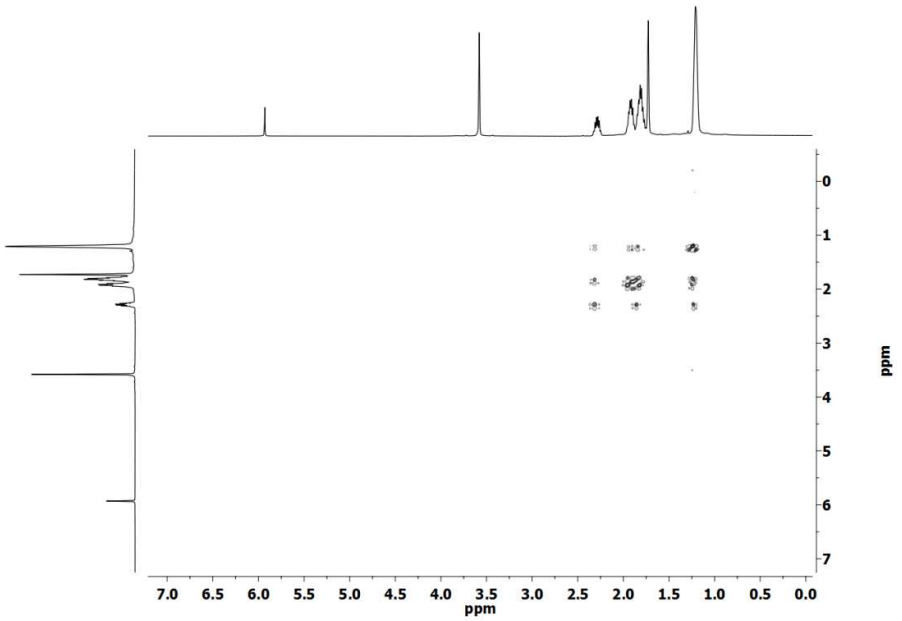

Figure S53. H,H Correlation (COSY) of **10** in THF-d_8

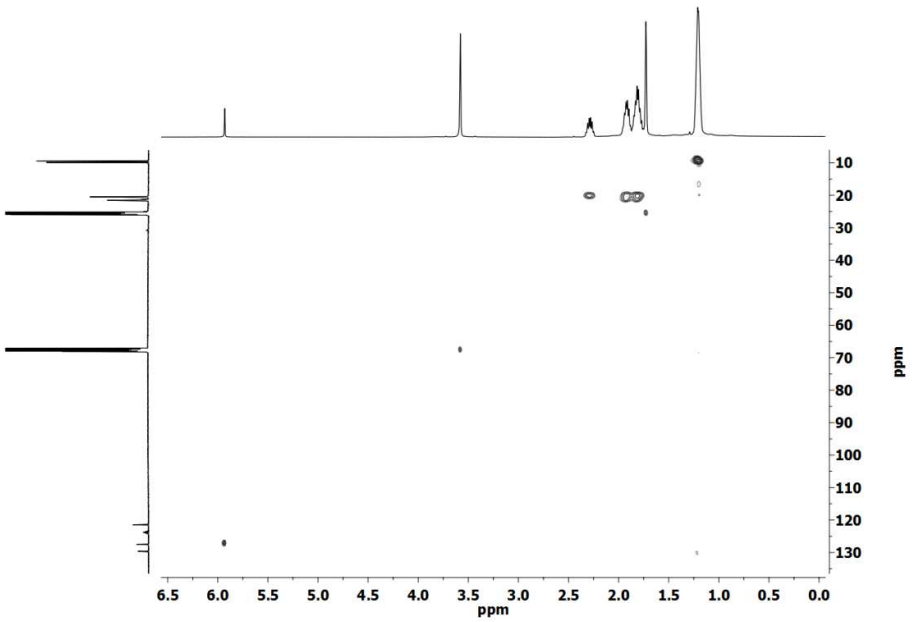

Figure S54. C,H Correlation of **10** in THF-d_8

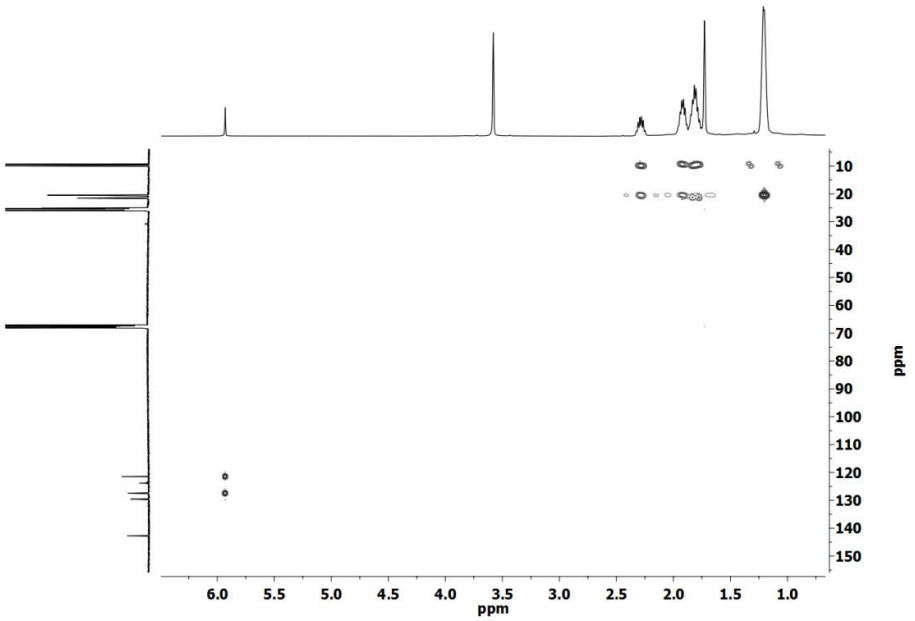

Figure S55. C,H Correlation (longrange) of **10** in THF-d_8

Infrared Spectra

Table S1. IR and Raman ν (C_4) bands of the bridging butadiyne unit of compounds **1** - **10**.

No.	IR [cm^{-1}] ν_{as} (C≡C)	IR [cm^{-1}] ν_{as} (C=C)	Raman [cm^{-1}] ν_s (C≡C)	Raman [cm^{-1}] ν_s (C=C)	ν (C≡N) [cm^{-1}]
1	2028 (vs)	1489 (m)	2030 (m)	1586 (s)	---
2	2036 (vs)	1571 (s), 1551 (m)	2040 (s)	1574 (m)	---
3	2023 (vs)	1595 (m), 1480 (s)	2040 (w)	1591 (vs)	---
4	2034 (s)	1502 (w)	2032 (m)	1439 (vs)	---
5	2046 (vs)	1551 (vs)	2049 (s)	1561 (m)	---
6	2044 (s)	1489 (m)	2043 (m)	1590 (s)	2092 (ν_{as}, s)
7	2041 (vs)	1574 (s), 1552 (m)	2040 (vs)	1578 (m), 1552 (w)	2092 (ν_{as}, s); 2097 (ν_s, m)
8	2034 (vs)	1596 (s), 1481 (s)	2045 (w)	1591 (vs), 1522 (vw)	2094 (ν_{as}, s)
9	2031 (s)	1503 (w)	2036 (m)	1434 (vs)	2094 (ν_{as}, s); 2097 (ν_s, w)
10	2043 (vs)	1552 (s)	2053 (vs)	1556 (m, br, sh at 1575)	2096 (ν_{as}, vs); 2101 (ν_s, m)

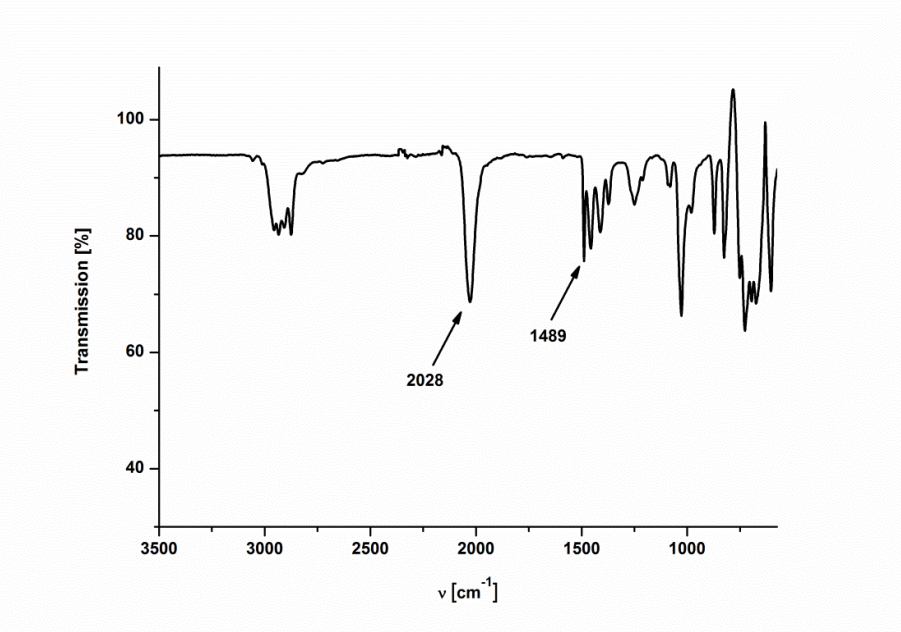

Figure S56. IR spectrum (ATR) of **1**

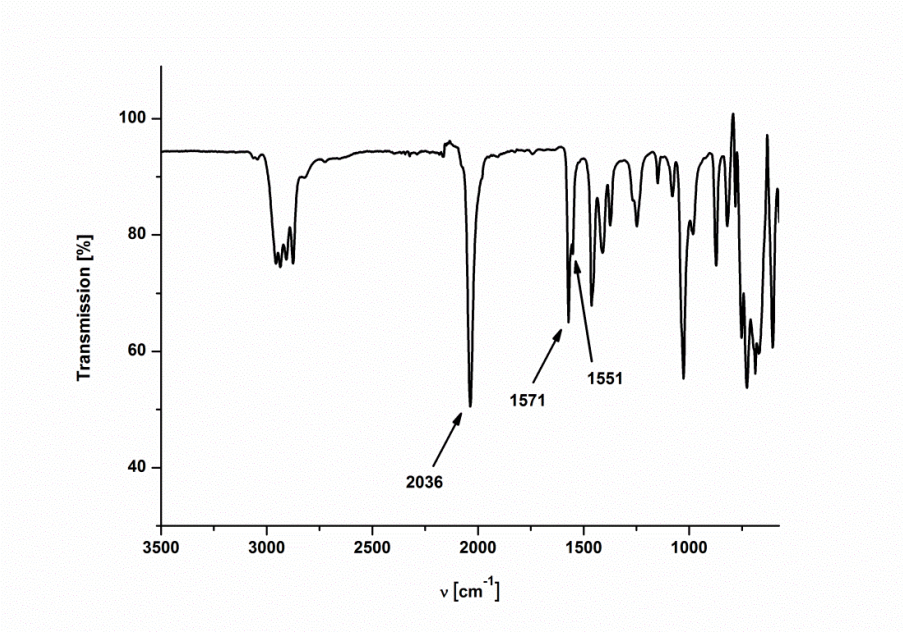

Figure S57. IR spectrum (ATR) of **2**

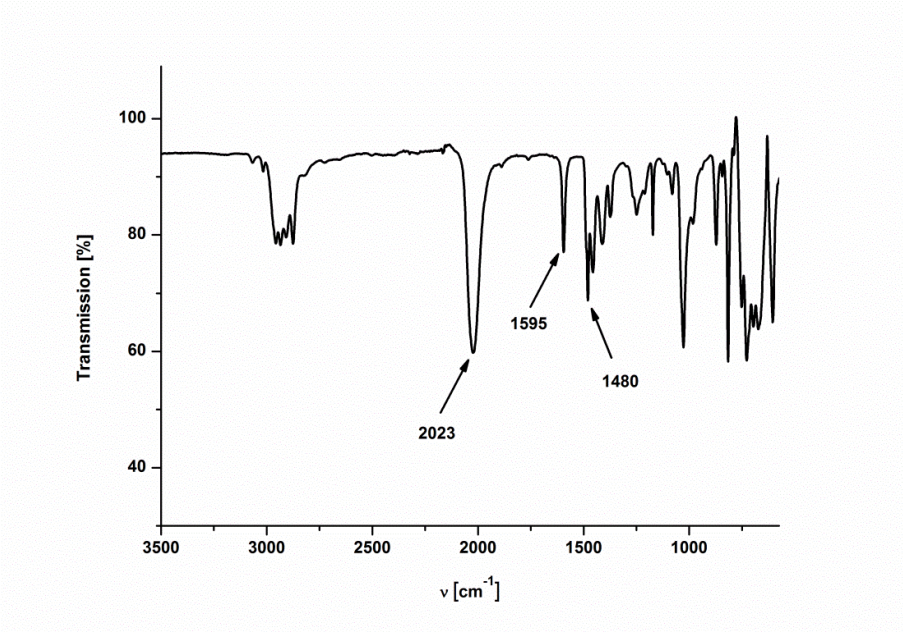

Figure S58. IR spectrum (ATR) of **3**

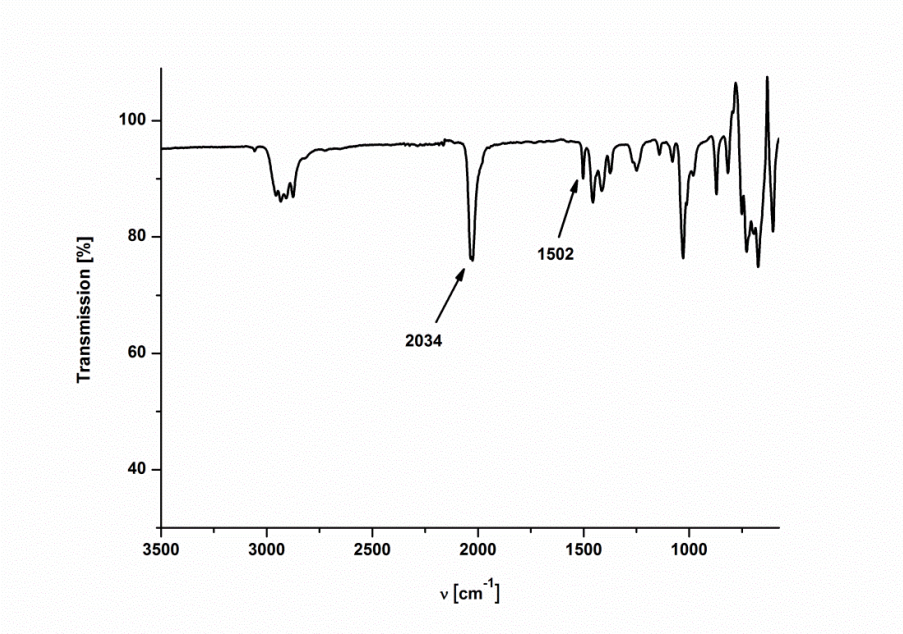

Figure S59. IR spectrum (ATR) of **4**

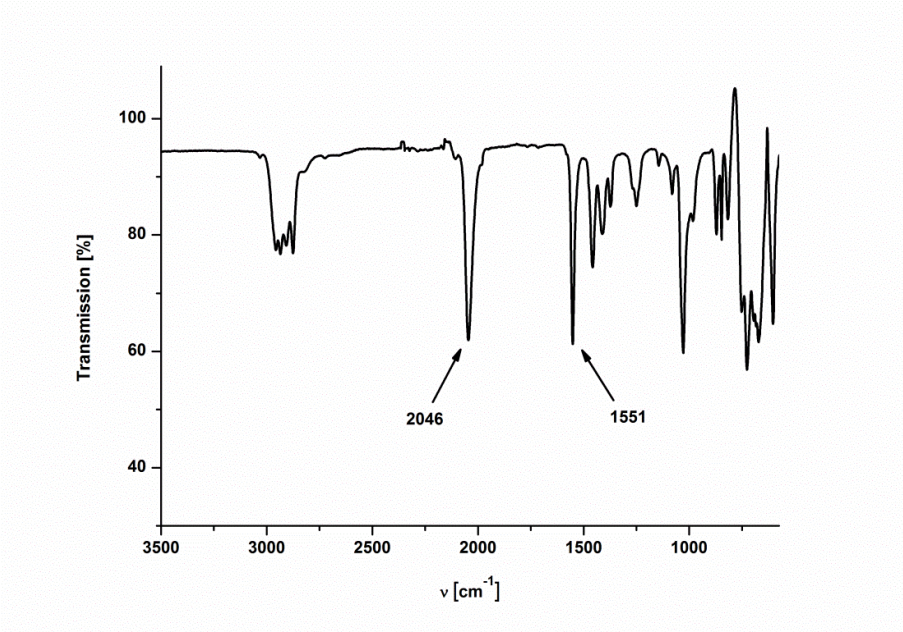

Figure S60. IR spectrum (ATR) of **5**

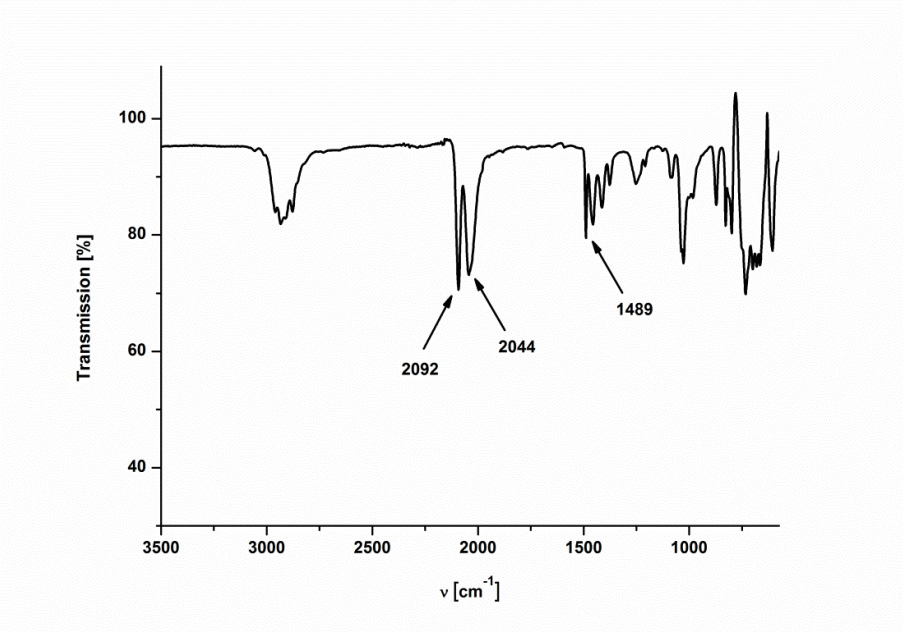

Figure S61. IR spectrum (ATR) of **6**

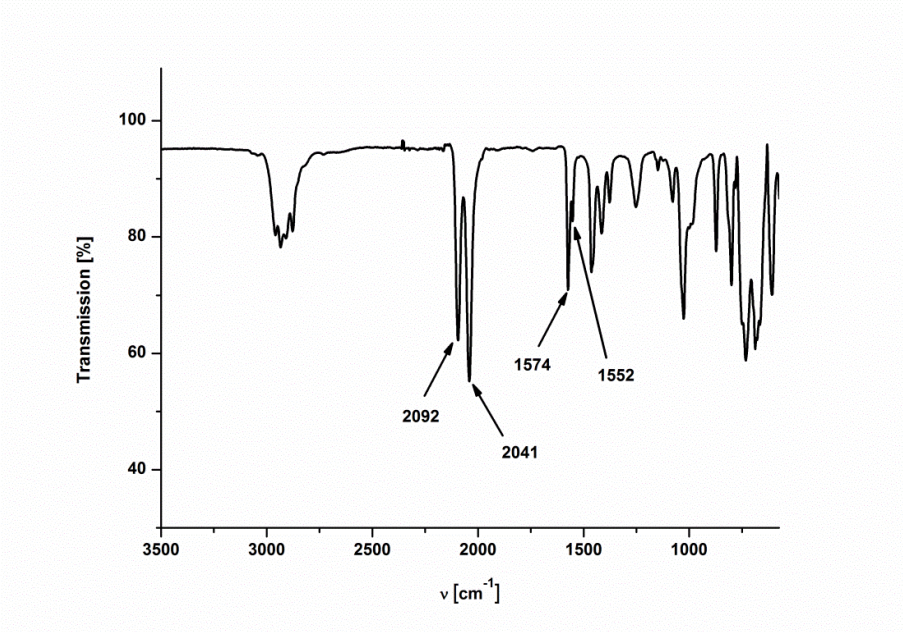

Figure S62. IR spectrum (ATR) of **7**

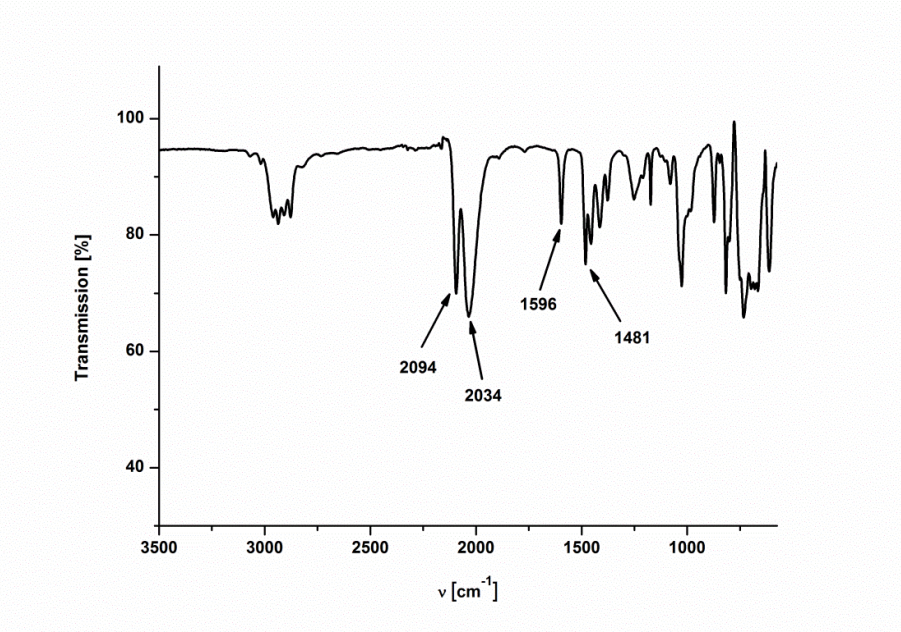

Figure S63. IR spectrum (ATR) of **8**

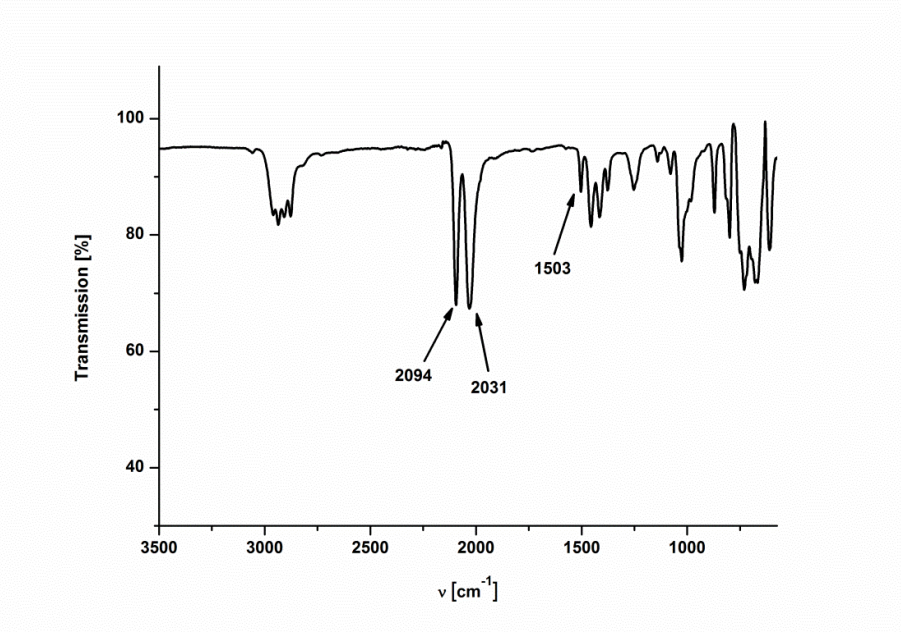

Figure S64. IR spectrum (ATR) of **9**

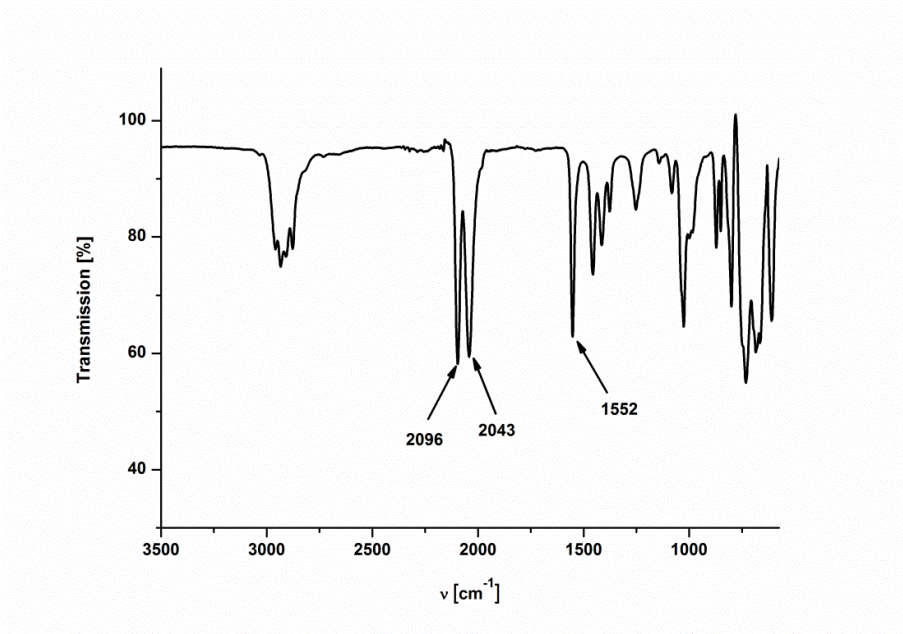

Figure S65. IR spectrum (ATR) of **10**

X-ray diffraction

Table S2. Crystallographic data for compounds **1**, **2** and **4**.

	1	**2**	**4**
empirical formula	$C_{50}H_{100}Fe_2I_2P_8$	$C_{50}H_{100}Fe_2I_2P_8$	$C_{48}H_{98}Fe_2I_2P_8S$
formula weight ($g \cdot mol^{-1}$)	1314.56	1314.56	1320.58
temperature (K)	153(2)	183(1)	153(2)
wavelength (Å)	0.71073	0.71073	0.71073
crystal system, space group	monoclinic, $P\,2_1/c$	monoclinic, $I\,2/a$	monoclinic, $P\,2_1/c$
a (Å)	16.5189(4)	16.1604(1)	12.1821(4)
b (Å)	9.9102(2)	13.9634(1)	29.8188(10)
c (Å)	18.2717(3)	27.1193(2)	19.5967(8)
α (deg)	90	90	90
β (deg)	97.748(2)	100.184(1)	124.521(3)
γ (deg)	90	90	90
volume ($Å^3$)	2963.87(11)	6023.17(7)	5865.2(4)
Z, density (calcd) ($Mg \cdot m^{-3}$)	2, 1.473	4, 1.450	4, 1.496
abs coefficient (mm^{-1})	1.779	1.750	1.832
F(000)	1356	2712	2720
crystal size (mm^3)	0.40 x 0.22 x 0.07	0.44 x 0.29 x 0.19	0.24 x 0.14 x 0.13
θ range (deg)	3.05 to 30.03	2.32 to 30.03	2.73 to 25.03
reflections collected	47537	62490	31417
reflections unique	8570 / R_{int} = 0.0459	8805 / R_{int} = 0.0325	10206 / R_{int} = 0.0371
completeness to θ (%)	98.9	100.0	98.3
absorption correction	analytical	semi-empirical from equivalents	analytical
max/min transmission	0.890 and 0.633	1.000 and 0.619	0.858 and 0.766
data / restraints / parameters	7514 / 2 / 308	8162 / 0 / 289	8009 / 74 / 518
goodness-of-fit on F^2	1.041	1.076	1.032
final R_1 and wR_2 indices [$I > 2\sigma(I)$]	0.0375, 0.0902	0.0235, 0.0602	0.0712, 0.1803
R_1 and wR_2 indices (all data)	0.0454, 0.0985	0.0263, 0.0625	0.0899, 0.1965
largest diff. peak and hole ($e \cdot Å^{-3}$)	2.722 and -1.061	0.745 and -0.588	1.790 and -1.777

The unweighted R-factor is $R_1 = \sum(Fo - Fc)/\sum Fo$; $I>2\sigma(I)$ and the weighted R-factor is $wR_2 = \{\sum w(Fo^2 - Fc^2)^2/\sum w(Fo^2)^2\}^{1/2}$

Table S3. Crystallographic data for compounds **5**, **6**, **8** and **9**.

	5	**6**	**8**	**9**
empirical formula	$C_{72}H_{147}Fe_3I_3P_{12}$, $0.5(C_6H_6)$	$C_{52}H_{100}Fe_2N_2P_8S_2$, $2(C_6H_5Cl)$	$C_{58}H_{104}Fe_2N_2P_8S_2$	$C_{50}H_{98}Fe_2N_2P_8S_3$
formula weight ($g \cdot mol^{-1}$)	1971.83	1402.02	1253.01	1182.98
temperature (K)	120(2)	183(1)	183(1)	183(1)
wavelength (Å)	1.54184	0.71073	0.71073	0.71073
crystal system, space group	monoclinic, $P\,2_1/c$	monoclinic, $P\,2_1/c$	orthorhombic, $P\,b\,c\,a$	monoclinic, $P\,2_1/c$
a (Å)	16.5273(5)	9.4939(6)	12.3808(2)	17.8328(4)
b (Å)	28.5966(10)	12.9379(5)	17.8464(2	20.0399(4)
c (Å)	20.0805(7)	29.598(2)	29.4377(4)	18.9596(4)
α (deg)	90	90	90	90
β (deg)	101.221(4)	90.369(6)	90	117.489(3)
γ (deg)	90	90	90	90
volume ($Å^3$)	9309.1(6)	3635.5(4)	6504.34(16)	6010.6(2)
Z, density (calcd) ($Mg \cdot m^{-3}$)	4, 1.407	2, 1.281	4, 1.280	4, 1.307
abs coefficient (mm^{-1})	13.729	0.744	0.744	0.834
$F(000)$	4068	1492	2680	2528
crystal size (mm^3)	0.20 x 0.10 x 0.03	0.30 x 0.11 x 0.04	0.45 x 0.34 x 0.04	0.35 x 0.07 x 0.01
θ range (deg)	2.72 to 68.25	2.56 to 25.35	2.12 to 30.40	2.37 to 28.78
reflections collected	50707	20403	43906	69260
reflections unique	17043 / R_{int} = 0.1258	6596 / R_{int} = 0.0696	8994 / R_{int} = 0.0286	13916 / R_{int} = 0.0582
completeness to θ (%)	99.9	98.9	100.0	99.9
absorption correction	semi-empirical from equivalents	analytical	analytical	analytical
max/min transmission	1.000 and 0.368	0.967 and 0.850	0.980 and 0.853	0.991 and 0.851
data / restraints / parameters	7144 / 128 / 248	4869 / 110 / 366	7387 / 36 / 371	10152 / 84 / 578
goodness-of-fit on F^2	1.114	1.021	1.023	1.131
final R_1 and wR_2 indices [$I > 2\sigma(I)$]	0.1298, 0.3467	0.0598, 0.1362	0.0392, 0.0920	0.1044, 0.2110
R_1 and wR_2 indices (all data)	0.2208, 0.4288	0.0865, 0.1536	0.0513, 0.0992	0.1383, 0.2259
largest diff. peak and hole ($e \cdot Å^{-3}$)	3.537 and -1.500	0.654 and -0.628	0.947 and -0.464	1.126 and -1.421

The unweighted R-factor is $R_1 = \sum(Fo - Fc)/\sum Fo$; $I>2\sigma(I)$ *and the weighted R-factor is* $wR_2 = \{\sum w(Fo^2 - Fc^2)^2/\sum w(Fo^2)^2\}^{1/2}$

***Table S4*.** Selected bond lengths [Å], non-bonding distances [Å] and angles [°] of compounds **1**, **2**, **4**, **6**, **8** and **9**.

	1	**2**	**4**	**6**	**8**	**9**
Space group	*P* 2_1/c	*I* 2/a	*P* 2_1/c	*P* 2_1/c	*P* bca	*P* 2_1/c
Bond lengths [Å]	**Fe1-C1** 1.883(2)	**Fe1-C1** 1.8862(14)	**Fe1-C1** 1.868(4) **Fe2-C8** 1.889(4)	**Fe1-C2** 1.899(4)	**Fe1-C2** 1.8991(16)	**Fe1–C22** 1.891(6) **Fe2-C29** 1.893(7)
	C1-C2 1.218(4)	**C1-C2** 1.220(2)	**C1-C2** 1.226(6) **C8-C7** 1.210(6)	**C2-C3** 1.221(5)	**C2-C3** 1.217(2)	**C22–C23** 1.220(9) **C29–C28** 1.211(10)
	C2-C3 1.433(3)	**C2-C3** 1.4329(19)	**C2-C3** 1.408(6) **C7-C6** 1.415(6)	**C3-C4** 1.441(5)	**C3-C4** 1.435(2)	**C23–C24** 1.417(9) **C28–C27** 1.424(9)
	Fe1-I1 2.6907(4)	**Fe1-I1** 2.7026(2)	**Fe1-I1A** 2.7146(9) **Fe2-I2A** 2.7065(9)	**Fe1-N1** 1.953(3)	**Fe1-N1** 1.9534(14)	**Fe1-N1** 1.965(6) **Fe2-N2** 1.964(6)
	---	---	---	**N1-C1** 1.160(5)	**N1-C1** 1.150(2)	**N1-C1** 1.119(8) **N2-C30** 1.121(8)
	---	---	---	**C1-S1** 1.645(4)	**C1-S1** 1.6405(18)	**C1-S1** 1.673(7) **C30-S2** 1.661(7)
	Fe-P 2.254(2) [a]	**Fe-P** 2.252(4) [a]	**Fe-P** 2.251(11) [a]	**Fe-P** 2.262(6) [a]	**Fe-P** 2.253(3) [a]	**Fe-P** 2.252(4) [a]
Non-bonding distances [Å]	**Fe1···Fe1'** 11.8981(2)	**Fe1···Fe1'** 9.7504(3)	**Fe1···Fe2** 11.1638(9)	**Fe1···Fe1'** 11.9343(10)	**Fe1···Fe1'** 16.2610(4)	**Fe1···Fe2** 11.2517(15)
	---	---	---	**S1···S1'** 21.4257(21)	**S1···S1'** 25.6847(11)	**S1···S2** 20.610(4)
Bond angles [°]	---	---	---	**S1-C1-N1** 179.7(4)	**S1-C1-N1** 178.85(18)	**S1-C1-N1** 177.9(6) **S2-C30-N2** 178.2(7)
	---	---	---	**C1-N1-Fe1** 173.5(3)	**C1-N1-Fe1** 176.56(15)	**C1-N1-Fe1** 173.1(5) **C30-N2-Fe2** 174.1(6)
	I1-Fe1-C1 176.98(8)	**I1-Fe1-C1** 178.90(4)	**I1A-Fe1-C1** 175.88(14) **I2A-Fe2-C8** 177.37(16)	**N1-Fe1-C2** 179.08(14)	**N1-Fe1-C2** 178.58(7)	**N1-Fe1-C22** 178.0(3) **N2-Fe2-C29** 177.1(3)
	Fe1-C1-C2 176.6(2)	**Fe1-C1-C2** 177.21(13)	**Fe1-C1-C2** 179.2(4) **Fe2-C8-C7** 176.2(4)	**Fe1-C2-C3** 177.4(3)	**Fe1-C2-C3** 177.61(16)	**Fe1-C22-C23** 179.1(6) **Fe2-C29-C28** 177.8(8)
	C1-C2-C3 176.5(3)	**C1-C2-C3** 172.67(15)	**C1-C2-C3** 176.0(4) **C8-C7-C6** 175.2(5)	**C2-C3-C4** 175.9(4)	**C2-C3-C4** 176.4(2)	**C22-C23-C24** 175.6(7) **C29-C28-C27** 177.3(9)

[a] Mean bond length: the estimated standard uncertainty *u* of the mean is calculated from the equation $u^2 = \frac{1}{n(n-1)} \sum_{i=1}^{n} (x^i - \bar{x})$ for a set of *n* values where x^i is the *i*th value and $\bar{x}$ is the mean of the n results considered.

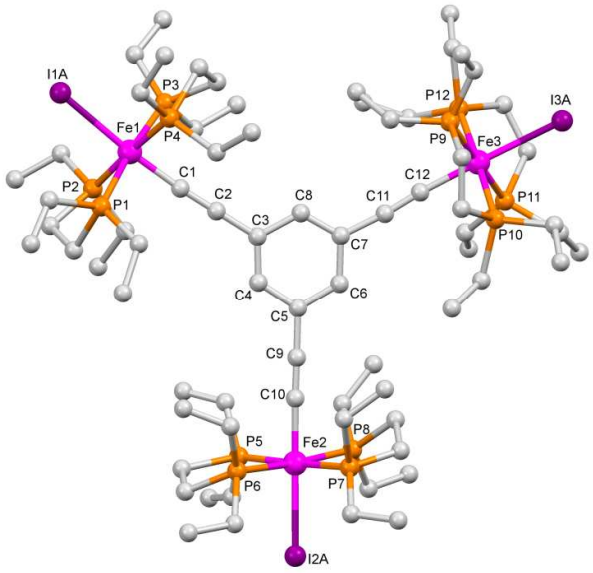

Figure S66. Molecular structures of: **5**. Solvent molecules and selected hydrogen atoms are omitted for clarity.

Refinement details.

In the crystal structure of **1**, one ethyl group is disordered over two sets of positions with site-occupancy factors of 0.253(9) and 0.747(9). Some bond distance restraints were used to correct the geometry of the disordered components. All non-hydrogen atoms were refined anisotropically. All hydrogen positions were calculated after each cycle of refinement using a riding model, with C—H = 0.93 Å and U_{iso}(H) = 1.2U_{eq}(C) for aromatic H atoms, with C—H = 0.97 Å and U_{iso}(H) = 1.2U_{eq}(C) for methylene H atoms, and with C—H = 0.96 Å and U_{iso}(H) = 1.5U_{eq}(C) for methyl H atoms.

In the crystal structure of **2**, the molecule lies on a two-fold rotation axis that passes through the substituted benzene ring (symmetry code: *i* = -*x*-1/2, *y*, -*z*). All non-hydrogen atoms were refined anisotropically. All hydrogen positions were calculated after each cycle of refinement using a riding model, with C—H = 0.93 Å and U_{iso}(H) = 1.2U_{eq}(C) for the aromatic H atoms, with C—H = 0.97 Å and U_{iso}(H) = 1.2U_{eq}(C) for the methylene H atoms, and with C—H = 0.96 Å and U_{iso}(H) = 1.5U_{eq}(C) for the methyl H atoms.

In the crystal structure of **4**, the main residue is disordered at 69% (as calculated in the checkCIF report). The central part of the molecule Fe-C_2-C_4H_2S-C_2-Fe is not disordered which makes the determination unambiguous. The selected crystal was clearly a monocrystal: 99.7% of the diffraction peaks fit with the cell parameters. No merohedral twinning is observed. The depe ligand containing P1 and P2 is partially disordered over two sets of positions with site-occupancy factors of 0.354(5) and 0.646(5), while the depe ligand containing P3 and P4 is fully disordered (except the P atoms) over two sets of positions with site-occupancy factors of 0.492(5) and 0.508(5). The depe ligands coordinated to Fe2 are fully disordered, P atoms included, with a relative occupancy of 0.414:0.586(2). The P6 and P8 atoms are also modeled with a 2-position disorder (despite a nearly perfect overlap of the atoms) in order to get bond distances and angles as reasonable as possible. The I atoms were also treated as disordered with site-occupancy ratios of 0.3973:0.6027(13) for I1 and 0.4508:0.5492(16) for I2. We did choose to disorder the I atoms to get rid of large residual peaks around the I positions (5.50 and 5.04 $e^-.A^{-3}$ at 1.46 and 0.90 Å from I1 and I2, respectively) which resulted in better final R values by about 3%. A total number of 74 restraints had to be used to correct the geometry of the disordered components of the molecule and the thermal parameters of the corresponding atoms. All non-hydrogen atoms were refined anisotropically. All hydrogen positions were calculated after each cycle of refinement using a riding model, with C—H = 0.93 Å and U_{iso}(H) = 1.2U_{eq}(C) for aromatic H atoms, with C—H = 0.97 Å and U_{iso}(H) = 1.2U_{eq}(C) for methylene H atoms, and with C—H = 0.96 Å and U_{iso}(H) = 1.5U_{eq}(C) for methyl H atoms.

In the crystal structure of **5**, only the main core of the molecule, $C_{12}Fe_3$, did not show any disorder. The whole molecule appeared clearly with most of the structure solution programs. Unfortunately, attemps to refine the model with a site-

occupancy of 1 for all atoms resulted to very large isotropic parameters. The *depe* ligand is well know to exhibit disorders, sometimes even all atoms of the ligand are disordered, it seems to be the case here for all three *depe* ligands. The fact that the crystal and the data collection were of a good quality, and that the non-disordered core confirms the expected molecule, we did refine the crystal structure of the compound to present the result in the Supporting Information (Appendix). First, the main core including the P and I atoms were freely refined, and then all C positions were located in Fourier difference maps, their xyz coordinates and isotropic parameters were fixed (U_{iso} = 0.08 for the ethane bridge C atoms, U_{iso} = 0.10 for the methylene C atoms of the ethyl groups, and U_{iso} = 0.015 for the methyl C atoms of the ethyl groups). Restraints had to be used to correct the geometry of some parts of the molecules, but we tried to check systematically bond distances and angles to unfix as many coordinates as possible. The Fe, I, P atoms as well as the central 12 C atoms were anisotropically refined. All hydrogen positions were calculated after each cycle of refinement using a riding model, with C—H = 0.93 Å and U_{iso}(H) = 1.2U_{eq}(C) for aromatic H atoms, with C—H = 0.97 Å and U_{iso}(H) = 1.2U_{eq}(C) for methylene H atoms, and with C—H = 0.96 Å and U_{iso}(H) = 1.5U_{eq}(C) for methyl H atoms.

In the crystal structure of **6**, the dinuclear species lies on an inversion center located in the middle of the central benzene ring (symmetry code: *i* = -*x*+1, -*y*, -*z*+1). It cocrystallized with solvent molecules of chlorobenzene in a ratio 1:2. The terminal CH_3 group of one ethyl ligand is disordered over two sets of positions with site-occupancy factors of 0.367(9) and 0.633(9). Some restraints had to be used to correct the geometry of the disordered parts and the thermal parameters of the corresponding atoms. All non-hydrogen atoms were refined anisotropically. All hydrogen positions were calculated after each cycle of refinement using a riding model, with C—H = 0.93 Å and U_{iso}(H) = 1.2U_{eq}(C) for aromatic H atoms, with C—H = 0.97 Å and U_{iso}(H) = 1.2U_{eq}(C) for methylene H atoms, and with C—H = 0.96 Å and U_{iso}(H) = 1.5U_{eq}(C) for methyl H atoms.

In the crystal structure of **8**, the dinuclear species lie on a center of inversion located in the middle of the central C—C bond. The second part of the molecule is obtained by a symmetry operation (-1-*x*, -*y*, -*z*). Two ethyl ligands are disordered over two sets of positions with site occupancy ratios of 0.495(8):0.505 (8) and 0.220(4):0.780 (4). All hydrogen positions were calculated after each cycle of refinement using a riding model, with C—H = 0.93 Å and U_{iso}(H) = 1.2U_{eq}(C) for aromatic H atoms, with C—H = 0.97 Å and U_{iso}(H) = 1.2U_{eq}(C) for methylene H atoms, and with C—H = 0.96 Å and U_{iso}(H) = 1.5U_{eq}(C) for methyl H atoms.

In the crystal structure of **9**, the diphosphine ligands bound to Fe2 are fully disordered over two sets of positions with a refined site-occupancy ratio of 0.413:0.587(4). Many restraints and constraints (84 *vs.* 584 parameters) had to be used to correct the geometry of the disordered components and the thermal parameters of the corresponding atoms. All hydrogen positions were calculated after each cycle of refinement using a riding model, with C—H = 0.93Å and U_{iso}(H) = 1.2U_{eq}(C) for aromatic H atoms, with C—H = 0.97Å and U_{iso}(H) = 1.2U_{eq}(C) for methylene H atoms, and with C—H = 0.96Å and U_{iso}(H) = 1.5U_{eq}(C) for methyl H atoms.

Cyclic Voltammetry Studies

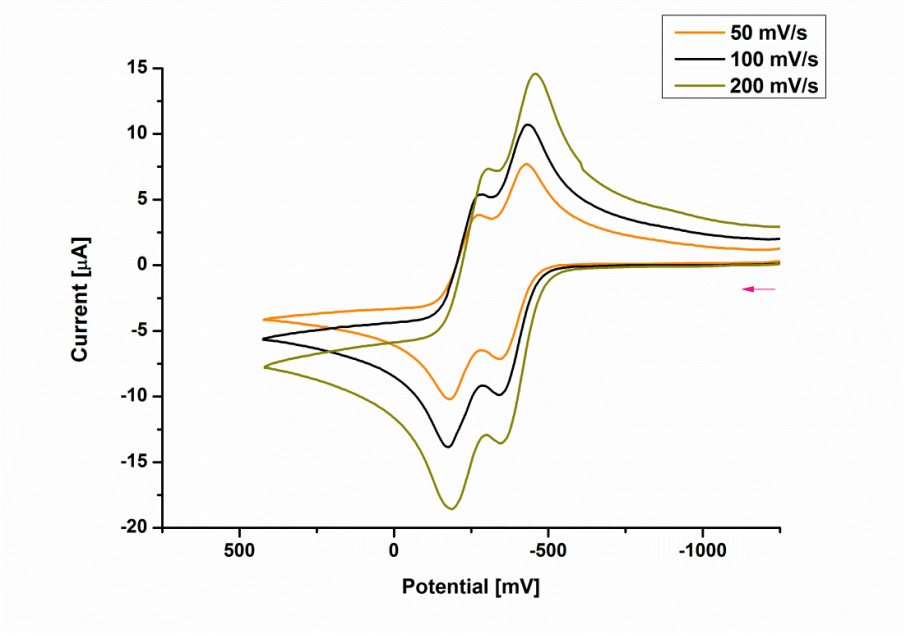

Figure S67. Cyclic voltammograms for **1** in NBu_4PF_6 (0.1M) at three different chart rates; rt, Au electrode; E vs. $Fc^{o/+}$ (external)

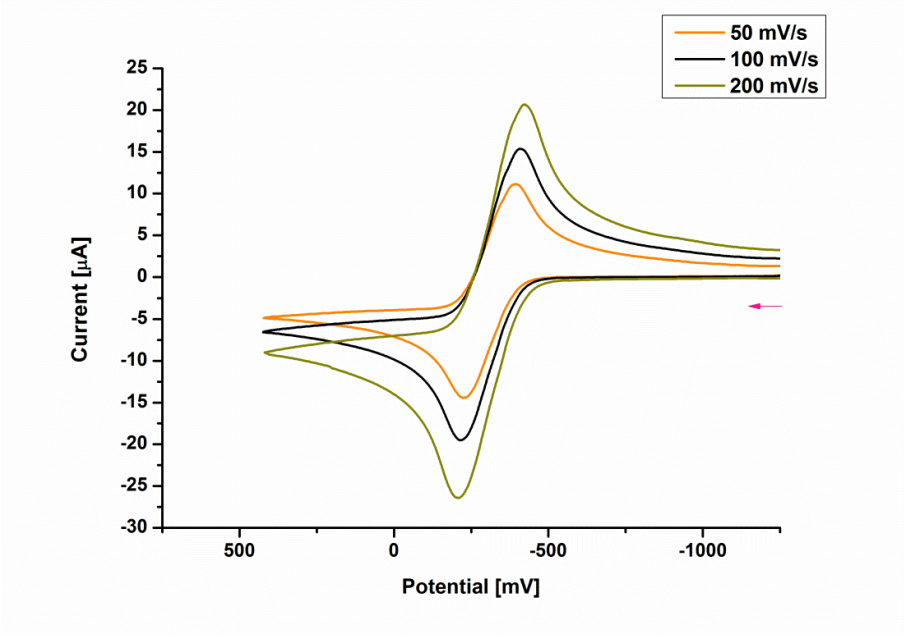

Figure S68. Cyclic voltammograms for **2** in NBu_4PF_6 (0.1M) at three different chart rates; rt, Au electrode; E vs. $Fc^{o/+}$ (external)

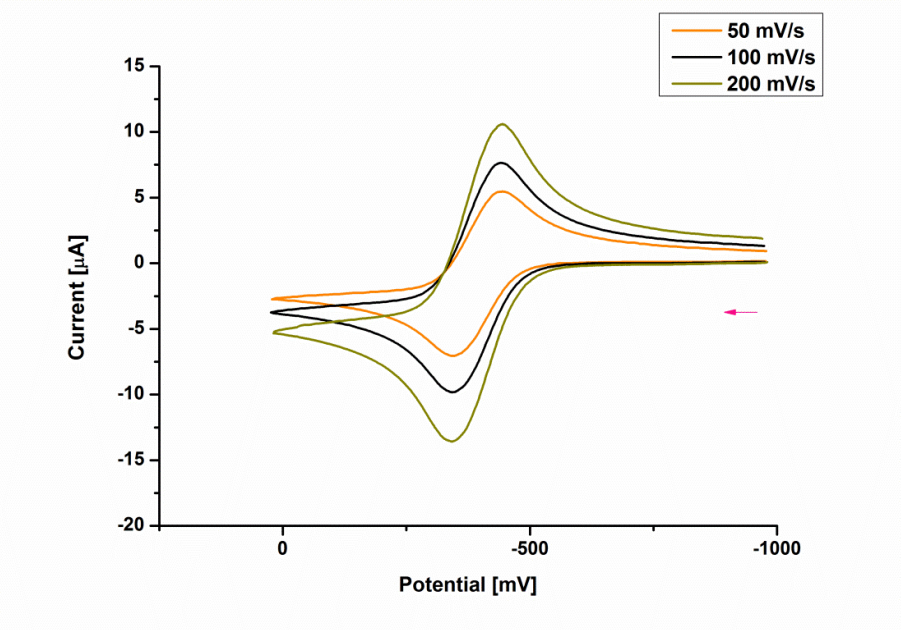

Figure S69. Cyclic voltammograms for **3** in NBu_4PF_6 (0.1M) at three different chart rates; rt, Au electrode; E vs. $Fc^{0/+}$ (external)

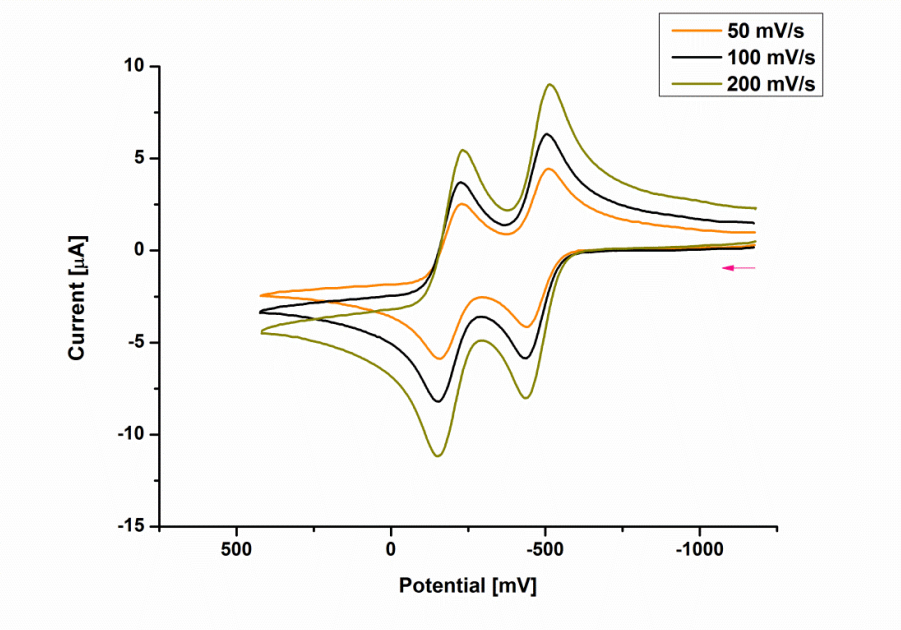

Figure S70. Cyclic voltammograms for **4** in NBu_4PF_6 (0.1M) at three different chart rates; rt, Au electrode; E vs. $Fc^{0/+}$ (external)

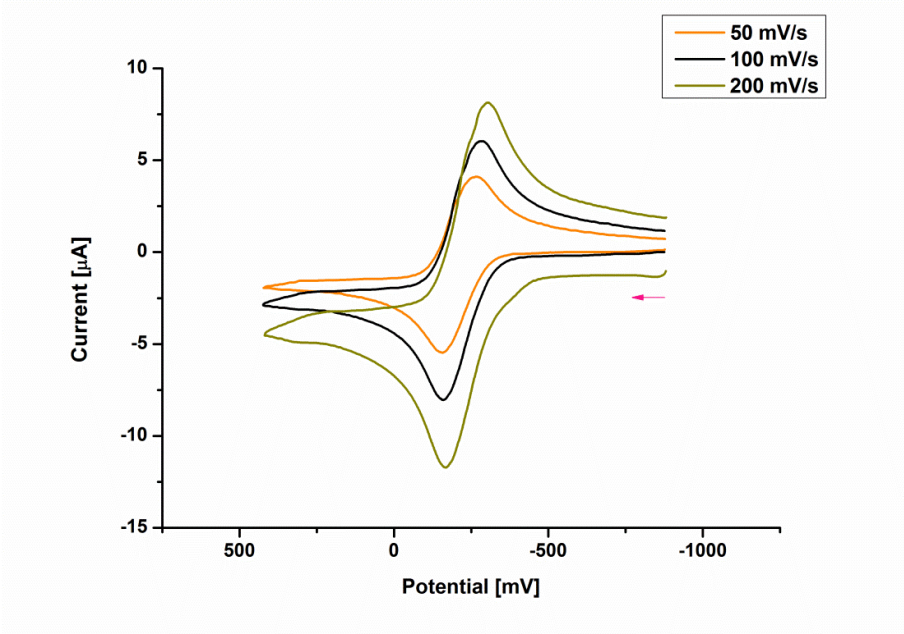

Figure S71. Cyclic voltammograms for **5** in NBu_4PF_6 (0.1M) at three different chart rates; rt, Au electrode; E vs. $Fc^{0/+}$ (external)

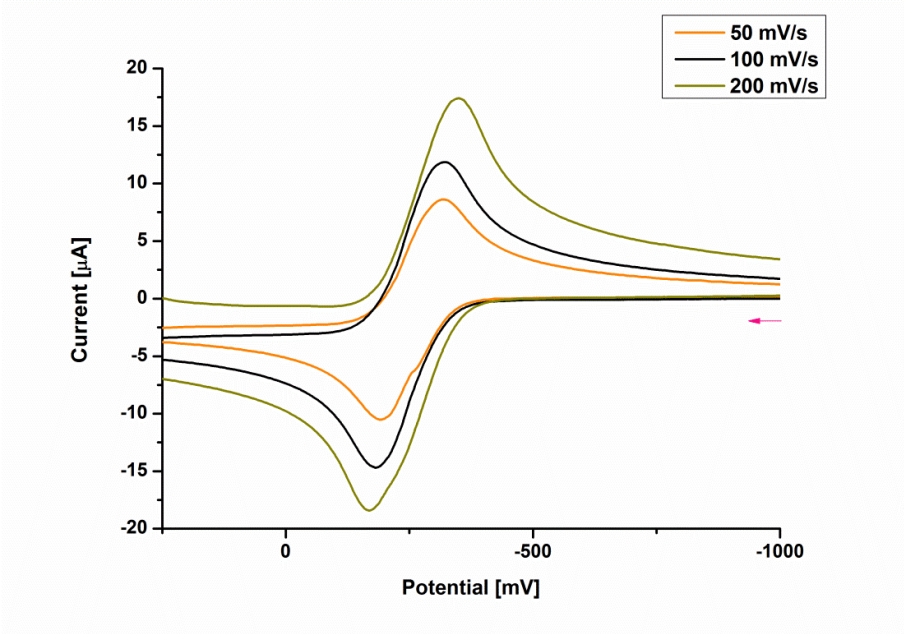

Figure S72. Cyclic voltammograms for **8** in NBu_4PF_6 (0.1M) at three different chart rates; rt, Au electrode; E vs. $Fc^{0/+}$ (external)

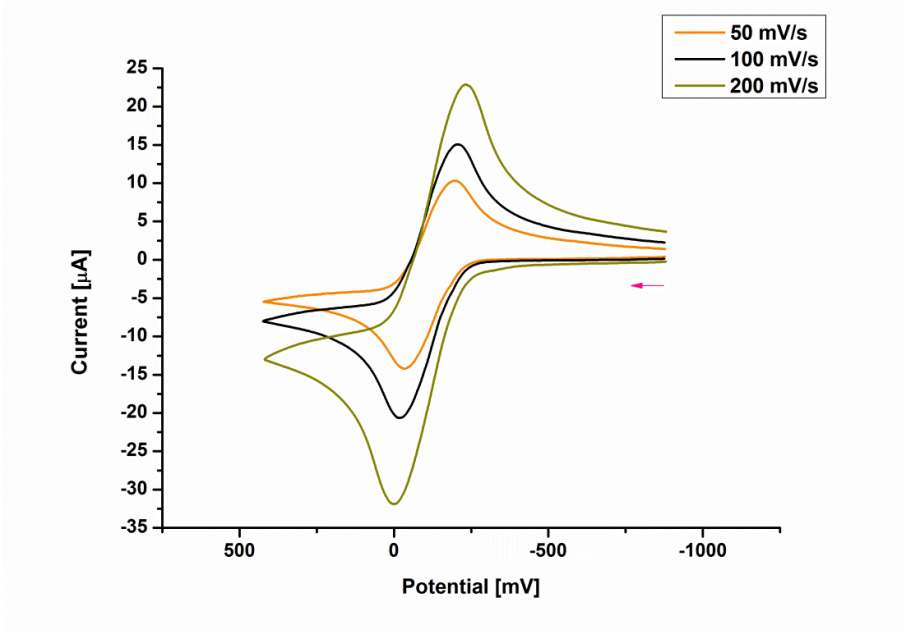

Figure S73. Cyclic voltammograms for **10** in NBu_4PF_6 (0.1M) at three different chart rates; rt, Au electrode; E vs. $Fc^{0/+}$ (external)

DFT Calculations

Table S5. Composition (%) of the HOMO of the calculated species model complexes **6**-*Me*, **7**-*Me*, **8**-*Me*, **9**-*Me* and of the C_4 bridged **C**-*Me* computed at the PBE1PBE/LANL2DZ//PBE1PBE/6-311+g(d) level.

	Fe	C_{α}	C_{β}	*bridge*	NCS
6	14	12	7	61	5
7	16	6	6	45	12
8	13	8	7	62	6
9	10	15	5	73	2
C	16	16	11	53	7

References

(1) Lissel, F.; Fox, T.; Blacque, O.; Polit, W.; Winter, R. F.; Venkatesan, K.; Berke, H. *J. Am. Chem. Soc.* **2013,** *135* (10), 4051–4060

(2) Fulmer, G. R.; Miller, A. J. M.; Sherden, N. H.; Gottlieb, H. E.; Nudelman, A.; Stoltz, B. M.; Bercaw, J. E.; Goldberg, K. I. *Organometallics*. **2010,** *29* (9), 2176–2179.